iography in mice by oral administration of ^{14}C-DEHP and observed that radioactivity levels of the intestinal wall, renal pelvis, bladder, urine, and liver reached their peaks at 4 hr after administration, and that they decreased afterwards except in the renal pelvis. In the present study, distribution of radioactivity observed as grains in testes and kidneys at 6 hr after administration of DEHP-^{3}H, significantly decreased at 24 hr after administration. Thus, DEHP or its metabolites distributed to testes and kidneys after single administration disappeared from the tissue rather fast. On the other hand, the grain count of the liver at 24 hr increased more than at 6 hr after administration, which suggests that DEHP or its metabolites were accumulated in the liver, possibly by enterohepatic circulation.

On autoradiography with oral administration of ^{3}H-DEHP, only a few radiosensitized grains were observed under light microscopic observation of thick sections of any tissues of the testes, liver or kidneys, and no grains were observed on electron microscopic autoradiography. This result implies that DEHP is rapidly splitted in the body into phthalic acid and alcohol, and only the phthalic acid moiety is transported into the tissues. It has been reported that orally administered phthalate diesters such as DEHP are rapidly changed in the gut to monoesters such as MEHP and absorbed, and that MEHP was similarly as potent as DEHP in causing testicular changes (Gray and Gangolli, 1986; Thomas and Thomas, 1984). On the other hand it has been reported that oral administration of phthalic acid did not cause testicular atrophy in rats (Cater *et al.*, 1977). From this and other experimental evidence, MEHP has been assumed to be the proximate toxicant (Albro *et al.*, 1989). In the present study, the radioactivity of DEHP labeled at the phthalic acid moiety penetrated the blood-testis barrier into Sertoli cells, while almost no tissue distribution of radioactivity were observed by autoradiography with DEHP labeled at the alcohol moiety (Fig. 1 and 2). Since MEHP metabolized from ^{3}H-DEHP was still radioactive, it is considered that orally administered DEHP was metabolized to MEHP before intestinal absorption and then further metabolized to the form of phthalic acid and taken into the testicular tissue. Thus, the phthalic acid moiety seems to be responsible for toxicological changes in testes. However, contradictory to the present results, Gray and Gangolli (1986) reported that ^{14}C-MEHP penetrated the blood-testis barrier only to a very limited extent. They used DEHP labeled with ^{14}C supposedly at the 7th position of phthalic acid or carbonyl carbon (Fig. 3). (They have not described the labeled position of the compound, but preceding papers had given the relevant information (Albro *et al.*, 1973; Schultz and Rubin, 1973).) It is chemically implausible that the carbonyl radical is detached so easily from the phthalic acid in the body. The conclusion of Gray and Gangolli (1986) that MEHP did not pass the blood-testis barrier was drawn from their observation that very little ^{14}C-MEHP appeared in rete testis fluid 25 min after intravenous administration. They remarked that MEHP affected Sertoli cells from the outside of the cells. The present study has demonstrated with autoradiography that the radioactivity of DEHP labeled at the phthalic acid moiety did pass the blood-testis barrier into Sertoli cells. Differences of test methods, amount of radioactivity used and timing of measurement may explain the discrepancy.

REFERENCES

Albro, P.W., Thomas, R. and Fishbein, L. (1973): Metabolism of diethylhexyl phthalate by rats. Isolation and characterization of urinary metabolites. J. Chromatogr., **76**, 321-330.

Albro, P.W., Chapin, R.E., Corbett, J.T., Schroeder, J. and Phelps, J.L. (1989): Mono-2-ethylhexyl phthalate, a metabolite of di-(2-ethylhexyl)phthalate, causally linked to testicular atrophy in rats. Toxicol. Appl. Pharmacol., **100**, 193-200.

Calley, D., Autian, J. and Guess, W.L. (1966): Toxicology of a series of phthalate esters. J. Pharm. Sci., **55**, 158-162.

Cater, B.R., Cook, M.W., Gangolli, S.D. and Grasso, P. (1977): Studies on dibutyl phthalate-induced testicular atrophy in the rat: Effect on zinc metabolism. Toxicol. Appl. Pharmacol., **41**, 609-618.

Creasy, D.M., Beech, L.M., Gray, T.J.B. and Butler, W.H. (1987): The ultrastructural effect of di-n-pentyl phthalate on the testis of the mature rats. Exp. Mol. Pathol., **46**, 357-371.

Creasy, D.M., Foster, J.R. and Foster, P.M.D. (1983): The morphological development of di-n-pentyl phthalate induced testicular atrophy in the rat. J. Pathol., **139**, 309-321.

Daniel, J.W. (1978): Toxicity and metabolism of phthalate esters. Clin. Toxicol., **13**, 257-268.

Gangolli, S.D. (1982): Testicular effects of phthalate esters. Environ. Health Perspect., **45**, 77-84.

Gaunt, I.F. and Butterworth, K.R. (1982): Autoradiographic study of orally administered di-(2-ethyl-

hexyl) phthalate in the mouse. Food Chem. Toxic., **20**, 215-217.

Gray, T.J. and Butterworth, K.R. (1980): Testicular atrophy produced by phthalate esters. Arch. Toxicol. Suppl., **4**, 452-455.

Gray, T.J., Butterworth, K.R., Gaunt, I.F., Grasso, G.P. and Gangolli, S.D. (1977): Short-term toxicity study of di-(2-ethylhexyl) phthalate in rats. Food Cosmet. Toxicol., **15**, 389-399.

Gray, T.J. and Gangolli, S.D. (1986): Aspects of the testicular toxicity of phthalate esters. Environ. Health Perspect., **65**, 229-235.

Saitoh, Y., Usumi, K., Nagata, T., Marumo, H., Imai, K. and Katoh, M. (1997) : Early changes in the rat testes induced by di-(2-ethylhexyl) phthalate and 2,5-hexandione – Ultrastructure and lanthanum trace study. J. Toxicol. Pathol., **10**, 51-57.

Schulz, C.O. and Rubin, R.J. (1973): Distribution, metabolism and excretion of di-2-ethylhexyl phthalate in the rat. Environ. Health Perspect., **3**, 123-129.

Thomas, J.A. and Thomas, M.J. (1984): Biological effects of di-(2-ethylhexyl) phthalate and other phthalic acid esters. Crit. Rev. Toxicol., **13**, 283-317.

Williams, D.T. and Blanchfield, B.J. (1974): Retention, excretion and metabolism of di-(2-ethylhexyl)phthalate administered orally to the rat. Bull. Environ. Contam. Toxicol., **12**, 109-112.

ELSEVIER

Bone 40 (2007) 876–887

BONE

www.elsevier.com/locate/bone

Effects of aromatase inhibitors on human osteoblast and osteoblast-like cells: A possible androgenic bone protective effects induced by exemestane

Yasuhiro Miki [a], Takashi Suzuki [a], Masahito Hatori [b], Katsuhide Igarashi [c], Ken-ich Aisaki [c], Jun Kanno [c], Yasuhiro Nakamura [a], Miwa Uzuki [d], Takashi Sawai [c], Hironobu Sasano [a,*]

[a] *Department of Pathology, Tohoku University Graduate School of Medicine, 2-1 Seiryo-machi, Aoba-ku, Sendai, Miyagi, 980-8575, Japan*
[b] *Department of Orthopedic Surgery, Tohoku University Graduate School of Medicine, Sendai, Japan*
[c] *Division of Toxicology, National Institute of Health Sciences, Biological Safety Research Center, Setagaya, Tokyo, Japan*
[d] *Department of Pathology, Iwate Medical College, Morioka, Japan*

Received 21 April 2006; revised 6 November 2006; accepted 14 November 2006
Available online 28 December 2006

Abstract

Effects of aromatase inhibitors (AIs) on the human skeletal system due to systemic estrogen depletion are becoming clinically important due to their increasing use as an adjuvant therapy in postmenopausal women with breast cancer. However, possible effects of AIs on human bone cells have remained largely unknown. We therefore studied effects of AIs including the steroidal AI, exemestane (EXE), and non-steroidal AIs, Aromatase Inhibitor I (AI-I) and aminoglutethimide (AGM), on a human osteoblast. We employed a human osteoblast cell line, hFOB, which maintains relatively physiological status of estrogen and androgen pathways of human osteoblasts, i.e., expression of aromatase, androgen receptor (AR), and estrogen receptor (ER) β. We also employed osteoblast-like cell lines, Saos-2 and MG-63 which expressed aromatase, AR, and ERα/β in order to further evaluate the mechanisms of effects of AIs on osteoblasts. There was a significant increment in the number of the cells following 72 h treatment with EXE in hFOB and Saos-2 but not in MG-63, in which the level of AR mRNA was lower than that in hFOB and Saos-2. Alkaline phosphatase activity was also increased by EXE treatment in hFOB and Saos-2. Pretreatment with the AR blocker, flutamide, partially inhibited the effect of EXE. AI-I exerted no effects on osteoblast cell proliferation and AGM diminished the number of the cells. hFOB converted androstenedione into E2 and testosterone (TST). Both EXE and AI-I decreased E2 level and increased TST level. In a microarray analysis, gene profile patterns following treatment with EXE demonstrated similar patterns as with DHT but not with E2 treatment. The genes induced by EXE treatment were related to cell proliferation, differentiation which includes genes encoding cytoskeleton proteins. We also examined the expression levels of these genes using quantitative RT-PCR in hFOB and Saos-2 treated with EXE and DHT and with/without flutamide. HOXD11 gene known as bone morphogenesis factor and osteoblast growth-related genes were induced by EXE treatment as well as DHT treatment in both hFOB and Saos-2. These results indicated that the steroidal aromatase inhibitor, EXE, stimulated hFOB cell proliferation via both AR dependent and independent pathways.

Keywords: Osteoblast; Aromatase inhibitor; Androgen; Estrogen; Exemestane

Introduction

Results in various epidemiological or clinical studies demonstrated that estrogens play important protective roles in human skeletal as well as cardiovascular systems, and estrogen deficiency resulted in accelerating the development of osteoporosis in postmenopausal women [1–3]. In breast cancer of postmenopausal women, hormone therapies without any clinically deleterious effects due to estrogen deficiency on bone metabolism as well as lipid metabolisms are preferable. Estrogen deficiency has been generally detected in the patients with breast cancer following chemotherapy induced ovarian failure, gonadotropin analogue, and aromatase inhibitors (AIs) therapy [4]. Aromatase is the pivotal enzyme of *in situ* or intratumoral estrogen biosynthesis in postmenopausal breast cancer patients, and catalyzes the conversion from androgens into estrogens (Fig. 1A). AIs therefore play an important role in

* Corresponding author. Fax: +81 22 273 5976.
E-mail address: hsasano@patholo2.med.tohoku.ac.jp (H. Sasano).

8756-3282/$ - see front matter © 2006 Elsevier Inc. All rights reserved.
doi:10.1016/j.bone.2006.11.029

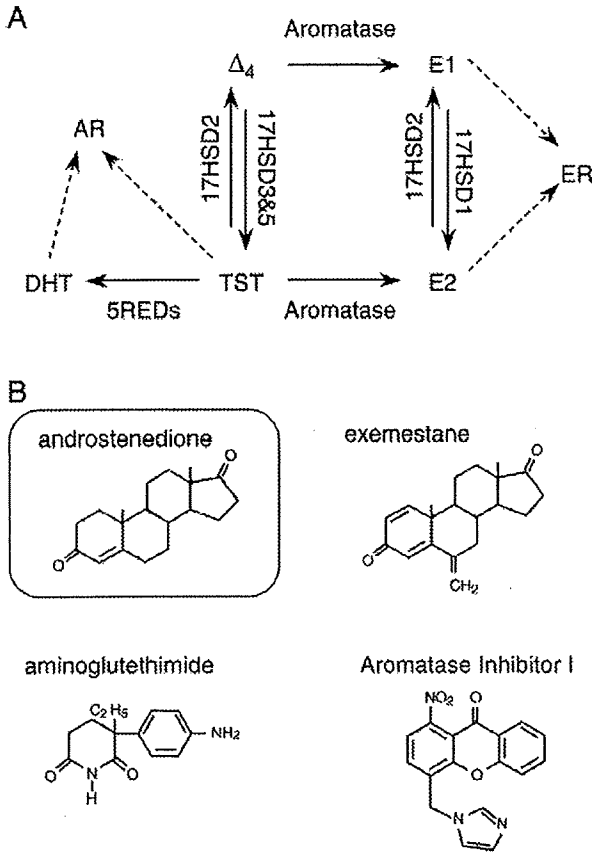

Fig. 1. (A) Summary of the pathway of estrogens and androgens production. Aromatase catalyzes the change from androstenedione (Δ4) and testosterone (TST) into estrone (E1) and estradiol (E2), respectively. 17HSD, 17β-hydroxysteroid dehydrogenase; 5REDs, 5α-reductase types 1 and 2; AR, androgen receptor; DHT, 5α-dihydrotestosterone; ER, estrogen receptor. (B) Structure of aromatase inhibitors used in this study. Androstenedione is a natural substrate of aromatase. Steroidal aromatase inhibitor, exemestane has an androstenedione-like structure.

clinical management of both primary and advanced breast cancer in postmenopausal women [5]. AIs are classified into two classes according to their modes of action. Type I AIs are steroidal inhibitions and one of them, exemestane (EXE) inhibits aromatase irreversibly and has an androstenedione (Δ_4)-like structure (Fig. 1B) [5–7]. Type II AIs are non-steroidal inhibitions and include aminoglutethimide (AGM), anastrozole, and letrozole [5].

Results of *in vivo* study using ovariectomized (OVX) rats demonstrated that EXE and its principal metabolite form, 17-hydroexemestane (17H-EXE) but not letrozole significantly prevented bone loss in OVX rats [8,9]. EXE and its principal metabolite, 17H-EXE, are structurally related to Δ_4 and bind to androgen receptor (AR) with relatively low affinity compared to 5α-dihydrotestosterone (DHT) [7]. These finding suggest that EXE may demonstrate protective effects toward bone tissues through its androgenic actions. However, detailed mechanisms of effects of EXE or androgen itself on human bone cells have remained largely unknown.

Various studies using human or animal bone tissues [10,11] and osteoblast cell culture using osteosarcoma cells [12,13] demonstrated that aromatase mRNA or protein was detected in osteoblast cells, which play an important role in bone remodeling. Therefore, in this study, we focused on effects of EXE in human osteoblast in an initial attempt to evaluate the effects of these AIs (summarized in Table 1 and Fig. 1B) [5–7,14], including AGM, EXE, and an experimental compound for inhibition of aromatase, Aromatase Inhibitor I (AI-I) [14] on human osteoblast and osteoblast-like cell lines. In our present study, we employed normal human cell line, hFOB, which maintains native characteristics of sex steroid hormone pathway of human osteoblasts, i.e., expression of AR, ERβ but not ERα, and aromatase. We also employed other osteoblast-like cell lines, Saos-2 and MG-63 which expressed ERα as well as ERβ in order to further study the mechanisms of effects of AI on human osteoblasts. We first examined the effects of estradiol (E2), DHT, progesterone (Prg), and AIs described above on cell proliferation of these cell lines, because the status of cell proliferation is important in the maintenance of homeostasis of bone tissue [15]. In addition, the effects of AIs on the conversion ratio of Δ_4 into E2 or testosterone (TST) in hFOB cultured medium were examined. We then screened E2, DHT, and EXE responsive genes using a microarray analysis in these cells, in order to further characterize the possible genomic effects of EXE on cell proliferation of osteoblasts. In this microarray analysis, hFOB was employed in order to examine the effects of E2, DHT, and EXE on native status of human osteoblasts but not on pathological status of osteoblasts such as osteosarcomas.

Materials and methods

Chemicals

Exemestane (EXE; FCE24304; 6-methyleneandrosta-1,4-diene-3,17-dione) and 17-hydroexemestane (17H-EXE; FCE25071; 6-methyleneandrosta-1,4-diene-17β-ol-3-one) were obtained from Pfizer, Inc. (MI, USA). Aminoglutethimide (AGM) and Aromatase Inhibitor I [AI-I; 4-(Imidazolylmethyl)-1-nitro-9*H*-9-xanthenone] were obtained from Sigma-Aldrich Co. (MO, USA) and EMD Biosciences, Inc. (CA, USA), respectively. Estradiol (E2), progesterone (Prg), and RU38,486 (RU; mifepristone), spironolactone were obtained from Sigma-Aldrich. ICI 182,780 (ICI; fulvestrant) and hydroxyflutamide (OHF) were obtained from Tocris Cookson Inc. (MO, USA) and Toronto Research Chemicals, Inc. (Ontario, Canada), respectively. 5α-dihydrotestosterone (DHT) was obtained from Wako Pure Chemical industries, Ltd. (Osaka, Japan).

Table 1
Aromatase inhibitors used in this study

	Aminoglutethimide	Exemestane	Aromatase inhibitor I
Trademark [a]	Cytadren®	Aromasin®	–
Type [b]	Type II	Type I	Type II
Generation	First	Third	–
IC50 (nM) [c]	3000	50	40

[a] Cytadren® is trademark of Novartis Pharmaseutical Corporation. Aromasin® is trademark of Pfizer Inc. Aromatase Inhibitor I is non-clinical compound of Calbiochem®.
[b] Type I is steroidal compound. Type II is a non-steroidal compound.
[c] Refs, Aminoglutethimide and Exemestane are Miller et al. [5]; Aromatase Inhibitor I is Recanatini et al. [14].

These materials were dissolved in pure ethanol (Wako Pure Chemical industries) and serially diluted (final concentrations: 10^{-12} M to 10^{-5} M), respectively. AGM was dissolved in DMSO (Wako Pure Chemical industries). The final concentration of ethanol and DMSO used in this study did not exceed 0.05%.

Osteoblast cell and osteoblast-like cell lines and culture conditions

Human normal osteoblast cell, hFOB 1.19 cell line (CRL-11372) was obtained from American Type Culture Collection (VA, USA). hFOB 1.19 cell was cultured according to the protocol previously described [16]. The cell line was maintained in a mixture of Dulbecco's Modified Eagle Medium and Ham's F12 medium (1:1) without phenol red (Invitrogen Corporation, CA, USA) supplemented with 10% fetal bovine serum (FBS; JRH Biosciences, KS, USA) and 50 mg/mL G 418 sulfate (EMD Biosciences). Human osteosarcoma cell lines Saos-2 and MG-63 were provided from the Cell Resource Center for Biomedical Research, Tohoku University (Sendai, Japan) and were maintained in a RPMI-1640 (Sigma-Aldrich) with 10% FBS. These cells were pre-incubated for 24 h with FBS-free medium prior to examination in order to remove exo-/endogenous steroid hormones from the culture medium and study the effects of various compounds in the absence of steroids and also to synchronize the cell cycle. Different concentrations of test compounds were added, and the assay was terminated after 3 or 5 days by removing the medium from wells. Steroid blockers were added simultaneously.

Characteristics of hFOB, Saos-2, and MG-63

Expressions of relevant steroid receptors, i.e., ERα, ERβ, and AR were determined using quantitative RT-PCR methods in hFOB, Saos-2, and MG-63 cell lines. mRNA transcripts of steroid synthesis/metabolite enzymes, aromatase, 17β-hydroxysteroid dehydrogenase (17β-HSD) types 1, 2, 3, 4, and 5, and 5α-reductase (5α-Red) types 1 and 2 were all evaluated using RT-PCR methods. The details of quantitative RT-PCR including primer sets employed were previously described in detail [17,18]. Positive controls for these receptors and enzymes were cell lines of human breast cancer, T-47D, and human prostate cancer, LNCaP obtained from Cell Resource Center for Biomedical Research, Tohoku University (Sendai, Japan). Alkaline phosphatase (ALP), an osteoblast-specific marker, was also studied using RT-PCR for characterization of these cell lines.

Estradiol and testosterone production assay

hFOB cells were plated in 10 mm dishes at a density of 10^6 viable cells and cultured for 48 h. Then media were changed to FBS-free medium, and hFOB cells were incubated with 10^{-7} M androstenedione (Δ_4; Sigma-Aldrich) in the presence or absence of EXE or AI-1 (10^{-7} M). The media were then collected after 24 h, and E2 and TST were measured by solid-phase radioimmunoassay. Radioimmunoassay was performed in SRL Inc. (Tokyo, Japan) using DPC estradiol kit and DPC total testosterone kit (Diagnostic Products Corporation, LA, USA). In addition, we confirmed that the concentrations of E2 and TST were under the detection limits (E2, 5 pg/mL; TST, 30 pg/mL) in the serum- and phenol red-free medium.

Cell proliferation assay

hFOB, Saos-2, and MG-63 cells were treated with steroids and test compounds for 24, 48, and 72 h, when specimens were harvested and evaluated for cell proliferation using the WST-8 method (Cell Counting Kit-8; Dojindo Inc., Kumamoto, Japan) [18]. Optical densities (OD, 450 nm) were evaluated using a SpectraMax 190 microplate reader (Molecular Devices, Corp., CA, USA) and Softmax Pro 4.3 microplate analysis software (Molecular Devices). The status of proliferation (%) was calculated according to the following equation: (cell OD value after test materials treated/vehicle control cell OD value) × 100.

Alkaline phosphatase activity assay

hFOB, Saos-2, and MG-63 cells were plated in 48 well plate at a density of 10^6 viable cells and cultured for 48 h. All cell lines were treated with 10^{-9} to 10^{-7} M exemestane for 72 h, when cells were lysed with 0.05% Triton X-100 (Wako Pure Chemical industries) and evaluated for alkaline phosphatase activity

Table 2
Primer sequences used in quantitative RT-PCR analysis

cDNA	GB#	Sequence	cDNA position	Size (bp)
MYBL2	NM_002466	Forward 5′-GTAACAGCCTCACGCCCAAGA-3′ Reverse 5′-TCCAATGTGTCCTGTTTGTTCCA-3′	1522–1615	94
OSTM1	NM_014028	Forward 5′-TTGAGAATAAGGCTGAACCTGGAAC-3′ Reverse 5′-TTACAGGCACTGTGTCACTGCAAG-3′	801–926	126
HOXD11[a]	NM_021192	Forward 5′-CAC TGT CCT TGG GTT TAA TG-3′ Reverse 5′-GGT AAA ATT GTA ACG GGA CG-3′	1091–1245	174
GPC2	NM_152742	Forward 5′-AGA AAT GTG GTC AGC GAA GC-3′ Reverse 5′-ACA CCT TCG CAC TGT TTT CC-3′	871-1183	313
ADCYAP1R1	NM_001118	Forward 5′-CAG CAA AAG GGA AAG ACT CG-3′ Reverse 5′-GAG CTG CTC TTG CTC AGG AT-3′	1351–1584	234
COL1A1	NM_000088	Forward 5′-GGT GGT GGT TAT GAC TTT GGT T-3′ Reverse 5′-CTT GGC TGG GAT GTT TTC AGG T-3′	3784–4092	309
SMAD1[a]	NM_005900	Forward 5′-GGT TCA CCT CAT AAT CCT-3′ Reverse 5′-CCT TTG TCA GTT CTC AAT C-3′	1779–1887	127
SMAD5[a]	NM_005903	Forward 5′-AGC TAA AGC CGT TGG ATA-3′ Reverse 5′-AGG CAC TAA TAC TGG AGG T-3′	668–768	119
RUNX2	NM_004348	Forward 5′-GTG GAC GAG GCA AGA GTT T-3′ Reverse 5′-TAC TGG GAT GAG GAA TGC G-3′	782–961	198
SPARC	NM_003118	Forward 5′-CCT GTA CAC TGG CAG TTC-3′ Reverse 5′-CCA GGG CGA TGT ACT TGT C-3′	793–937	163
ALP	NM_000478	Forward 5′-ACC ATT CCC ACG TCT TCA CA-3′ Reverse 5′-AGA CAT TCT CTC GTT CAC CGC C-3′	1379–1540	162
RPL13A	NM_012423	Forward 5′-CCT GGA GGA GAA GAG GAA AGA GA-3′ Reverse 5′-TTG AGG ACC TCT GTG TAT TTG TCA A-3′	487–612	126

GB#, GeneBank accession number.
All primer sets were designed using OLIGO Primer Analysis Software (TAKARA Bio Inc., Shiga, Japan).
[a] Forward and reverse primers were located in sama exon.

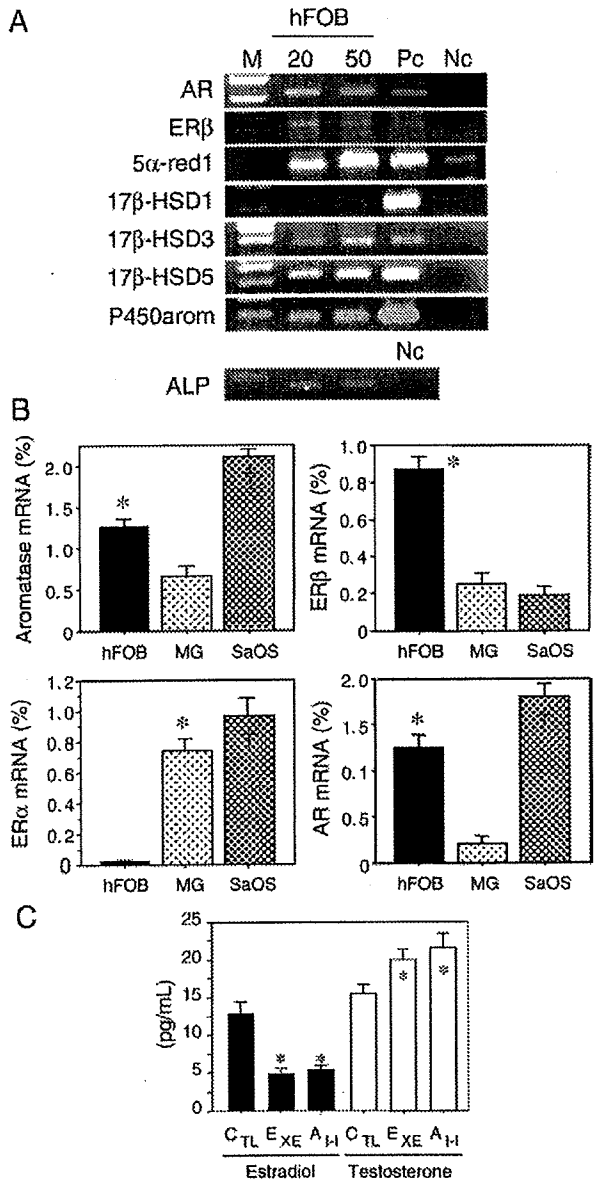

Fig. 2. (A) Results of RT-PCR analysis of steroid hormone receptors and steroid-related enzymes. Both 20 and 50 ng/μL cDNA of hFOB were used for PCR (ALP was 20 ng/μL alone). AR, androgen receptor; ER, estrogen receptor; 5α-red1, 5α-reductase type 1; 17β-HSD, 17β-hydroxysteroid dehydrogenase; P450 arom, aromatase; M, molecular marker; Pc, positive control; Nc, negative control. (B) Expression levels of aromatase, AR, ERα, and ERβ in hFOB, Saos-2, and MG-63. *$p<0.05$ vs. MG-63 (aromatase and AR), vs. MG-63 and vs. Saos-2 (ERβ), vs. hFOB (ERα); †$p<0.05$ vs. hFOB and MG-63 (aromatase and AR), vs. MG-63 and hFOB (ERα). (C) Estradiol and testosterone productions in hFOB cells. The data are expressed as the mean SD ($n=3$). *$p<0.05$ vs. control cells (CTL). EXE, 10^{-7} M exemestane; AI-I, 10^{-7} M aromatase inhibitor I.

using the *p*-nitrophenylphosphate method (LabAssay ALP; Wako Pure Chemical industries) [19]. Optical densities (OD, 405 nm) were evaluated using a SpectraMax 190 microplate reader (Molecular Devices) and Softmax Pro 4.3 microplate analysis software (Molecular Devices). ALP activity (units/μL) = (concentration of *p*-nitrophenol/15 min) × 1 (dilution factor of sample). The ALP activities were presented as units/μL/10^6 cells. The ALP activity levels in each case were represented as a ratio of vehicle control (%).

Microarray analysis

The procedure was based on a previously reported study [20]. Cell lysates were prepared using RLT buffer (QIAGEN GmbH, Hilden, Germany). Total RNA was extracted using RNeasy Mini Kit (QIAGEN). First-strand cDNA was synthesized by incubating 5 μg of total RNA with 200 U SuperScript II reverse transcriptase (Invitrogen), 100 pmol T7-(dT)24 primer (Invitrogen). Ten units of T4 DNA polymerase (Invitrogen) were then added, and the dsDNA was mixed with T7 RNA polymerase (Invitrogen). The purified cRNA was fragmented at 300–500 bp as target solution. Hybridization was performed with the GeneChip Human Genome 133 ver. 2.0 (Affymetrix, Inc., CA, USA). The reacted arrays were then scanned as digital image files and scanned data were analyzed with GeneChip software (Affymetrix). Relative levels of gene expression were calculated by global normalization.

Data were subjected to hierarchical clustering analysis and visualization using the Cluster and TreeView programs (Stanford University) in order to generate tree structures based on the degree of similarity, as well as matrices comparing the levels of expression of individual genes in each sample [21].

Real-time PCR

Real-time PCR was carried out using the LightCycler System and the FastStart DNA Master SYBR Green I (Roche Diagnostics GmbH, Mannheim, Germany). The primer sequences used in this study are summarized in Table 2. An initial denaturing step of 95 °C for 10 min was followed by 35 cycles, respectively, at 95 °C for 10 min; 15 s annealing at 65 °C (ALP, COL1A1), 64 °C (MYBL2, OSTM1, RPL13A), 62 °C (SMAD1, SMAD5, SPARC, RUNX2), or 60 °C (HOXD11); and extension for 15 s at 72 °C. Negative control experiments included those lacking cDNA substrates to confirm the presence of exogenous contaminant DNA. No amplified products were detected under these conditions. The mRNA levels in each case were represented as a ratio of RPL13A (%) [22].

Immunohistochemistry of AR

Five non-pathological bone tissues were retrieved from surgical pathology files (two females and three males, 17 to 55 years old) of Department of Pathology, Tohoku University Hospital (Sendai, Japan).

Tissue sections were immunostained using a biotin-streptavidin method with Histofine kit (Nichirei Co. Ltd., Tokyo, Japan). The monoclonal antibody for AR (AR411) [23] was obtained from DakoCytomation (Kyoto, Japan). Experimental procedures employed in our present study have been previously described in detail [22,23]. The dilutions of primary AR antibody were 1:100. The antigen-antibody complex was then visualized with 3,3′-diaminobenzidine solution, and counterstained with hematoxylin. Prostate cancer was used as a positive control for AR. Normal mouse IgG was used as a negative control for immunostaining and no specific immunoreactivity was detected.

Statistical analysis

Results were expressed as mean±SD. Statistical analysis was performed with the StatView 5.0 J software (SAS Institute Inc., NC, USA). All data were analyzed by analysis of variance (ANOVA) followed by post hoc Bonferroni/Dunnett multiple comparison test. A p-value <0.05 was considered to indicate statistical significance.

Results

Characteristics of hFOB, MG-63, and Saos-2 cell line

Characteristics of osteoblast and osteoblast-like cell lines are summarized in Figs. 2A and B. hFOB cells expressed mRNA transcripts of AR and ERβ. Relatively low level of ERα mRNA transcript was detected in hFOB cells. Aromatase, 17β-HSD type 1, 3, and 5, and 5α-Red types 1 and 2 mRNA transcripts were all detected in hFOB cells by

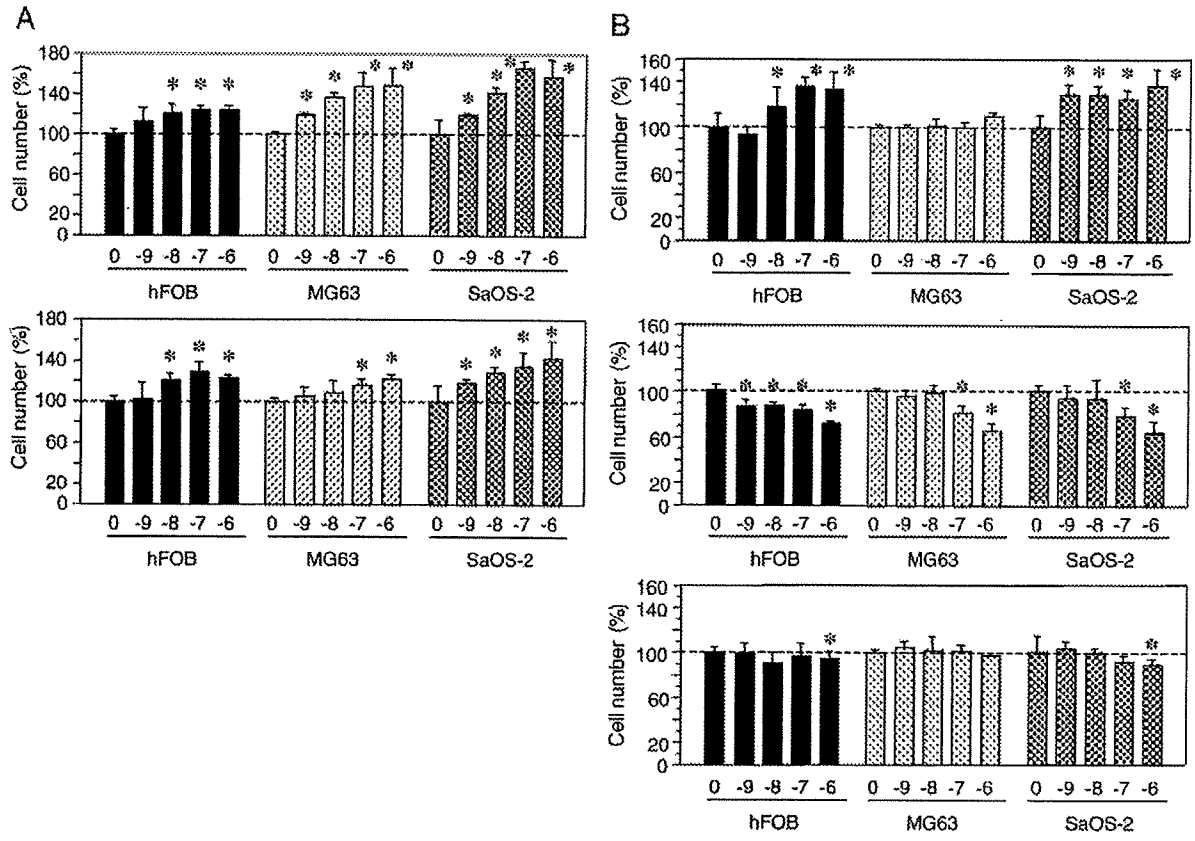

Fig. 3. (A) Proliferation of hFOB cells treated by estradiol (top) and 5α-DHT (bottom). *$p<0.05$ vs. vehicle control (0). (B) Proliferation of hFOB cells treated by exemestane (top), aminogluthetimide (middle), and Aromatase Inhibitor-I (bottom). *$p<0.05$ vs. vehicle control (0). $n=5$.

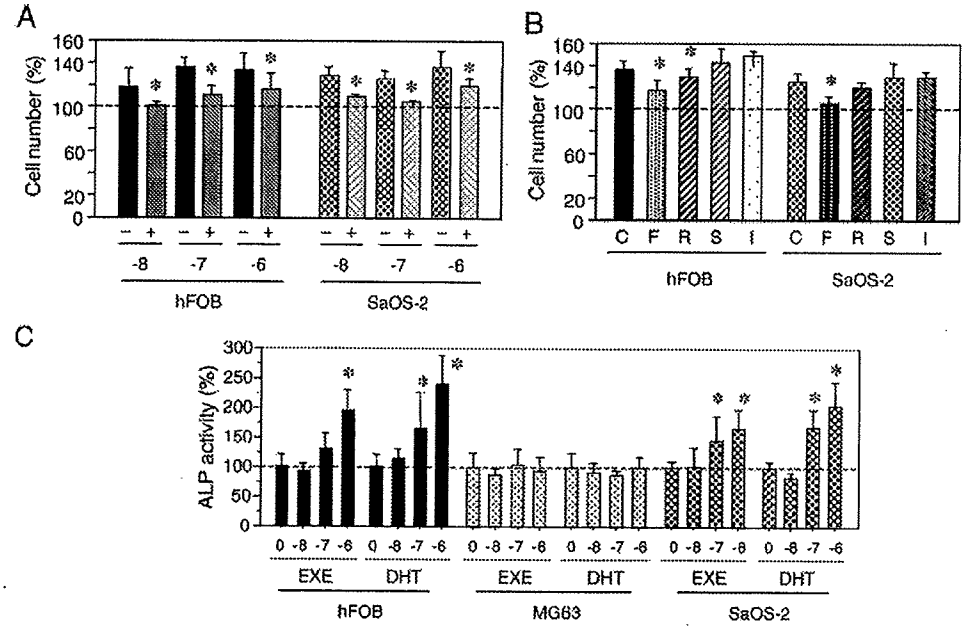

Fig. 4. (A) Effects of hydroxyflutamide on exemestane (10^{-8} to 10^{-6} M) stimulated the cell proliferation of both hFOB and Saos-2. With (+) or without (−) hydroxyflutamide, $p<0.05$ vs. without hydroxyflutamide (*). (B) Effects of steroid receptor blockers on exemestane (10^{-7} M) stimulated cell proliferation of hFOB and Saos-2. C, 10^{-7} M exemestane; F, hydroxyflutamide (5×10^{-6} M); R, RU38,486 (5×10^{-6} M); S, spironolactone (5×10^{-6} M); I, ICI182,720 (5×10^{-6} M). *$p<0.05$ vs. C (C) ALP activity in hFOB, Saos-2, MG-63 treated with exemestane (EXE, 10^{-8} to 10^{-6} M), or 5α-DHT (DHT, 10^{-8} to 10^{-6} M). *$p<0.05$ vs. vehicle control (0).

RT-PCR. Aromatase, ERα, ERβ, and AR were all detected in osteoblast-like cell lines, Saos-2 and MG-63 (Fig. 2B). In hFOB cell, expression of ERβ mRNA was more predominant than that of ERα mRNA. ERα mRNA as well as ERβ mRNA was detected in Saos-2 and MG-63 cells. The levels of AR mRNA expression in both hFOB and Saos-2 were significantly higher (p=0.01) than that in MG-63. ALP mRNA was also detected in intact hFOB, Saos-2, and MG-63 cells (data not present), respectively.

Estradiol and testosterone production

Results were summarized in Fig. 2C. The E2 levels in the medium of hFOB supplemented with Δ_4 treated with EXE or AI-I were significantly lower than that of cells without AIs. The levels of TST in the medium of hFOB supplemented with Δ4 treated with EXE or AI-I were significantly higher than that of cells without AIs.

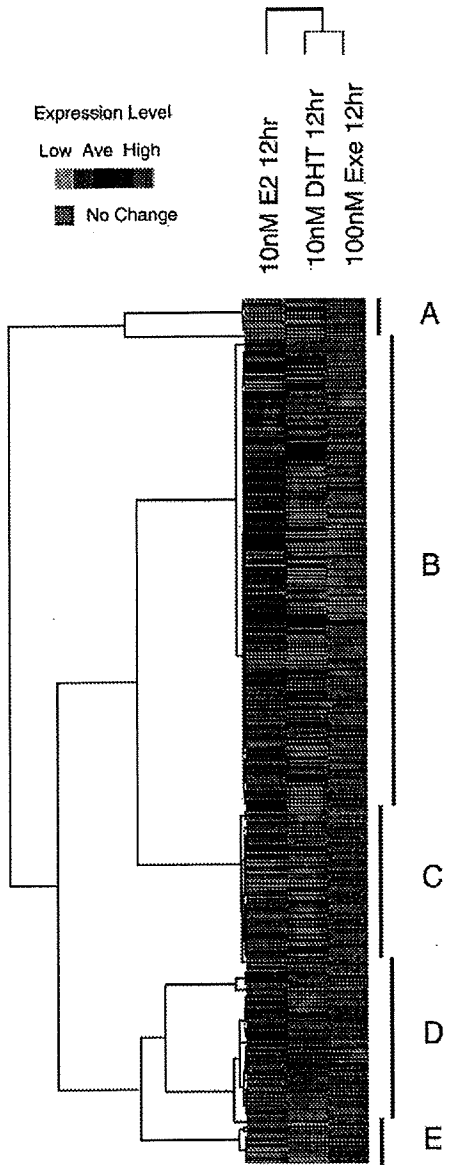

Fig. 5. In clustering analysis of the expression levels of each gene in hFOB cells treated with estradiol (E2), 5α-dihydrotestosterone (DHT), and exemestane (Exe).

Cell proliferation

Results of the cell proliferation assays are summarized in Figs. 3 and 4. There was a significant increment in the number of the cells after 72 h in hFOB, Saos-2, and MG-63 cells treated with 10^{-9} M (Saos-2 and MG-63) or 10^{-8} M (hFOB) to 10^{-6} M E2 (Fig. 3A). The cell number of hFOB and Saos-2 cells treated by 10^{-9} M (Saos-2) or 10^{-8} M (hFOB) to 10^{-6} DHT for 72 h was also significantly higher than control (Fig. 3A). The number of MG-63 cells was significantly increased only by high dose of DHT (10^{-7} M and 10^{-6} M) treatments (Fig. 3A). Prg (10^{-9} M to 10^{-6} M) treatments did not change the number of cells even after 72 h in all three cell lines examined (data not present).

Both EXE (Fig. 3B) and 17H-EXE (data not present) treatments of 10^{-8} M to 10^{-6} M, which were comparable to pharmacological inhibition doses of aromatization (Table 1), significantly increased the hFOB cell number for 72 h, respectively. In Saos-2 cells treated with relatively low dose, 10^{-9} to 10^{-6} M EXE, there was a significant increment in the number of the cells after 72 h (Fig. 3B). However, all the dose (10^{-9} M to 10^{-6} M) of EXE employed did not results in the change of cell number of MG-63 even after 72 h of treatment (Fig. 3B). The cell number of both hFOB and Saos-2 cells treated by both 10^{-6} M EXE and/or 17H-EXE for 48 h was also significantly higher than that treated for 24 h (data not present).

AGM treatment [10^{-9} (hFOB) or 10^{-7} (Saos-2 and MG-63) to 10^{-6} M] diminished the number of these three cells (Fig. 3B) and morphological changes in these cells were consistent with those caused by cytotoxic effects (data not present). AI-I treatment (10^{-9} to 10^{-7} M) was not associated with significant increment of the cell number in these cell lines (Fig. 3B). Only high dose (10^{-6} M) of AI-I significantly diminished the cell numbers of hFOB and Saos-2 but not of MG-63 (Fig. 3B).

The androgen receptor antagonist OHF (5×10^{-6} M) diminished the effects of EXE on these increments of both hFOB and Saos-2 cells (Figs. 4A and B). Treatment with RU but not spironolactone and ICI also inhibited EXE effects on hFOB cells (Fig. 4B).

ALP activity assay

Results of the ALP activity assay were summarized in Fig. 4C. There was a significant increment in the ALP activity of both hFOB and Saos-2 cells treated with 10^{-7} M (Saos-2) and/or 10^{-6} M (hFOB and Saos-2) EXE. Both 10^{-7} M and 10^{-6} M DHT treatment also increased the ALP activity in hFOB and Saos-2 cells, respectively. There were no changes of ALP activity in MG-63 treated with 10^{-8} M to 10^{-6} M of EXE and DHT, respectively.

Table 3a
Genes induced by exemestane treatment in hFOB cells—2.0 higher

	Gene title	Gene symbol	Raw data			Ratio	
			C	D	Ex	D	Ex
NM_002466	V-myb myeloblastosis viral oncogene homolog (avian)-like 2	**MYBL2**	70.9	156.9	150.3	2.2	2.1
AW444985	–	–	57.8	124.7	127.1	2.2	2.2
AF143684	Myosin IXB	MYO9B	48.3	64.4	122.2	1.3	2.5
NM_024682	TBC1 domain family, member 17	TBC1D17	31.7	37.6	64.8	1.2	2.0
BE965311	Chromosome 16 open reading frame 23	C16orf23	29.2	44.2	64.0	1.5	2.2
NM_004233	CD83 antigen (activated B lymphocytes, immunoglobulin superfamily)	CD83	29.0	66.5	60.9	2.3	2.1
AI806031	Skeletal muscle and kidney enriched inositol phosphatase	SKIP	27.7	48.6	55.4	1.8	2.0
AL136729	Ring finger protein 123	RNF123	20.0	23.7	41.3	1.2	2.1
NM_015254	Kinesin family member 13B	KIF13B	13.0	24.5	39.4	1.9	3.0
AL110249	Chromosome 20 open reading frame 194	C20orf194	13.4	39.0	29.7	2.9	2.2
AF208502	Early B-cell factor	EBF	12.5	21.1	28.5	1.7	2.3
AW007221	Solute carrier family 13 (sodium/sulfate symporters), member 4	SLC13A4	12.3	9.6	27.8	0.8	2.3
AB007458	TP53 activated protein 1	TP53AP1	12.6	22.2	26.2	1.8	2.1
AV713913	Osteopetrosis associated transmembrane protein 1	**OSTM1**	9.8	16.5	21.3	1.7	2.2
BF339201	THAP domain containing 6	THAP6	6.0	14.0	20.6	2.3	3.4
AK000455	Hypothetical gene MGC16733 similar to CG12113	MGC16733	7.3	16.6	18.8	2.3	2.6
AW974816	–	–	2.2	16.0	17.2	7.2	7.7
AK025325	Transcribed locus, moderately similar to NP_689573.2 zinc finger protein 573	–	7.3	11.4	16.2	1.6	2.2
NM_021192	Homeo box D11	**HOXD11**	5.3	16.2	15.8	3.0	3.0
NM_022169	ATP-binding cassette, sub-family G (WHITE), member 4	ABCG4	7.0	10.5	15.7	1.5	2.2
R62907	Disabled homolog 2, mitogen-responsive phosphoprotein (*Drosophila*)	DAB2	7.7	13.0	15.5	1.7	2.0
NM_002661	Phospholipase C, gamma 2 (phosphatidylinositol-specific)	PLCG2	7.3	12.3	15.3	1.7	2.1
BG393032	Solute carrier family 13 (sodium/sulfate symporters), member 4	SLC13A4	6.4	6.7	15.1	1.0	2.3
BC002794	Tumor necrosis factor receptor superfamily, member 14	TNFRSF14	6.2	11.3	13.6	1.8	2.2
BC042908	KIAA0690	KIAA0690	5.6	7.4	13.5	1.3	2.4
AW451961	Adenylate cyclase activating polypeptide 1 (pituitary) receptor type 1	**ADCYAP1R1**	4.3	11.7	13.2	2.7	3.1
AI863264	Glypican 2 (cerebroglycan)	**GPC2**	5.3	7.2	13.2	1.3	2.5
AF130050	ACA47 scaRNA gene	-	5.6	9.5	12.9	1.7	2.3
AK022326	Hypothetical gene supported by AK022326	-	6.1	12.7	12.9	2.1	2.1
AK021807	Low density lipoprotein receptor-related protein 11	LRP11	5.9	6.2	12.8	1.0	2.2
AU155415	Kallikrein 7 (chymotryptic, stratum corneum)	KLK7	5.6	13.5	12.7	2.4	2.3
BF673779	Hypothetical protein FLJ30834	FLJ30834	5.5	6.3	12.3	1.1	2.2
AV646335	–	–	2.6	13.0	11.2	5.0	4.3
BC040600	–	–	5.0	5.4	10.6	1.1	2.1
AI131035	–	–	5.1	9.2	10.5	1.8	2.1

C, vehicle control; D, 5α-dihydrotestosterone; Ex, exemestane. Genes that performed quantitative RT-PCR were described in bold style.

Microarray/clustering analysis

In hFOB cells, the hierarchical clustering analysis contains 430 genes which demonstrated expression ratios above 2.0-fold and below 0.5-fold compared with vehicle control cells after 12 h of each gene treated with 10^{-8} M E2, 10^{-8} M DHT, or 10^{-7} M EXE. The expression profiles of EXE treated cells were closely related to those of DHT (Fig. 5). In this study, we focused on 35 genes (Table 3a), which were all up-regulated twice or more than control. In this group, we further focused on 5 genes, B-Myb 2 (MYBL2), osteopetrosis associated transmembrane protein 1 (OSTM1), homeo box D 11 (HOXD11), adenylate cyclase activating polypeptide 1 receptor (ADCYAP1R1), and glypican 2 (GPC2) which are all considered to play important roles in EXE or DHT induced cell proliferation. We therefore examined whether these 5 genes were increased by EXE or DHT treatments using quantitative RT-PCR in hFOB cells. We also examined the validation of results of microarray analysis obtained in hFOB cells in Saos-2 and MG-63 cells.

Validation of microarray analysis using quantitative RT-PCR

In hFOB cells, all of these 5 genes described above were significantly increased by 10^{-7} M EXE treatment, and 3/5 genes (except for OSTM1 and GPC2) were also significantly increased by 10^{-8} M DHT treatment. HOXD11 and ADCYAP1R1 genes increased by both EXE and DHT were significantly diminished by OHF (5×10^{-6} M) treatment (Figs. 6A–C).

The similar results of changes of MYBL2 expression were also obtained in both Saos-2 and MG-63 treated with EXE and DHT, respectively (Fig. 6A). In addition, the results of HOXD11 expression in hFOB were equivalent to those in Saos-2 but not in MG-63 treated with EXE and DHT (Fig. 6B). Other genes induced by treatment of EXE and DHT in hFOB such as OSTM1, GPC2, and ADCYAP1R1 were not changed in both Saos-2 and MG-63 cells treated with EXE and DHT, respectively (data not present). AI-I or AGM treatment did not increase all of these genes expression in hFOB (data not present).

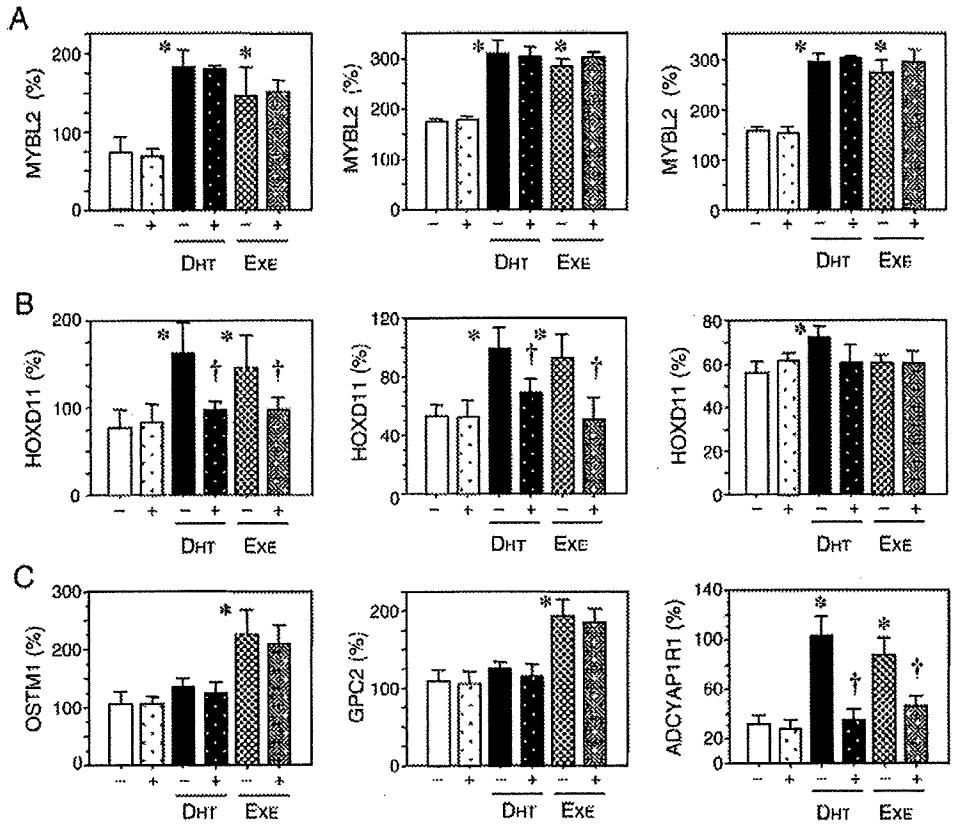

Fig. 6. Validation of microarray analysis. (A) Expression levels of MYBL2 in hFOB (left), Saos-2 (middle), and MG-63 (right). (B) Expression levels of HOXD11 in hFOB (left), Saos-2 (middle), and MG-63 (right). (C) Expression levels of OSTM1, GPC2, and ADCYAP1R1 in hFOB. DHT: 10^{-8} M 5α-dihydrotestosterone, EXE: 10^{-7} M Exemestane, with (+) or without (−) hydroxyflutamide, $p<0.05$ vs. control (*) or without hydroxyflutamide (†).

Analysis of osteoblast growth-related genes

Results of microarray analysis in hFOB cell demonstrated that osteoblast growth-related genes [24,25] such as COL1A1, SMAD1, SMAD5, SPARC, and RUNX2 were all up-regulated by exemestane (10^{-7} M) treatment but the degrees of increment were all under 2-fold (Table 3b). In this microarray analysis, other expression levels of previously reported osteoblast-related genes were not altered.

In hFOB cells, the validation analysis of these genes described above using quantitative RT-PCR (Fig. 7) demonstrated that 4/5 genes (except for COL1A1) were significantly increased by 10^{-7} M EXE treatment, and 4/5 genes (except for SMAD1) were also significantly increased by 10^{-8} M DHT treatment. The increased expression of the SMAD1, SMAD5, and SPARC genes by EXE or DHT, was significantly diminished by OHF (5×10^{-6} M) treatment. There were no effects of OHF pretreatment on the increased expression levels of RUNX2 that had occurred after both EXE and DHT treatments. Both AI-I and AGM treatment could not increase all of these genes expression in hFOB (data not present).

In Saos-2 cells, 4/5 genes (except for RUNX2) were significantly increased by 10^{-7} M EXE treatment, and 3/5 genes (except for RUNX2 and SMAD1) were also significantly increased by 10^{-8} M DHT treatment. The increment of the COL1A1, SMAD5, and SPARC genes expression by EXE or DHT, was significantly diminished by OHF (5×10^{-6} M) treatment. All of these 5 genes did not change in MG-63 cells treated with EXE or DHT, respectively (data not present).

Immunohistochemistry of AR

Marked AR immunoreactivity was detected in the nuclei of osteoblasts or lining cells but not in osteoclasts in four cases (Fig. 8). In these four cases, AR immunoreactivity was also detected in osteocytes and condrocytes. In one case, there was no immunoreactivity in all types of bone cells.

Discussion

In the clinical study of EXE compared to placebo administrated for two years [26,27], EXE modestly enhanced bone loss from the femoral neck without significant influence on lumber bone loss despite a marked systemic estrogen depletion. Furthermore, the risks of clinical bone fractures are considered to be lower with EXE treatment than that seen with non steroidal AIs [27,28], though it is also important to recognize that EXE has not been shown to significantly increase the amount of bone mass in various clinical studies of breast cancer patients [26,27]. The relative protective effect of EXE, a

Table 3b
Genes induced by exemestane treatment in hFOB cells—the osteoblast growth-related genes

	Gene title	Gene symbol	Raw data			Ratio	
			C	D	Ex	D	Ex
K01228	Collagen, type I, alpha 1	**COL1A1**	2797.2	3240.9	3058.5	1.2	1.1
BE221212	Collagen, type I, alpha 1	**COL1A1**	2741.1	3048.3	3052.2	1.1	1.1
AI743621	Collagen, type I, alpha 1	**COL1A1**	228.0	241.6	242.5	1.1	1.1
AA788711	Collagen, type I, alpha 2	COL1A2	2250.6	2474.3	2375.4	1.1	1.1
NM_000089	Collagen, type I, alpha 2	COL1A2	1749.1	1848.7	1787.6	1.1	1.0
M60485	Fibroblast growth factor receptor 1	FGFR1	178.9	185.7	198.6	1.0	1.1
BE467261	Fibroblast growth factor receptor 1	FGFR1	165.4	208.6	189.7	1.3	1.1
M63889	Fibroblast growth factor receptor 1	FGFR1	119.3	111.6	140.5	0.9	1.2
NM_023110	Fibroblast growth factor receptor 1	FGFR1	60.5	84.0	70.2	1.4	1.2
AU145411	Fibroblast growth factor receptor 1	FGFR1	29.2	44.1	37.5	1.5	1.3
AI359368	Fibroblast growth factor receptor 3	FGFR3	41.4	65.5	58.7	1.6	1.4
NM_001552	Insulin-like growth factor binding protein 4	IGFBP4	809.1	1027.5	1040.4	1.3	1.3
AL353944	Runt-related transcription factor 2	**RUNX2**	192.9	226.3	216.3	1.2	1.1
AU146891	SMAD, mothers against DPP homolog 1 (*Drosophila*)	**SMAD1**	161.2	195.6	204.6	1.2	1.3
NM_005901	SMAD, mothers against DPP homolog 2 (*Drosophila*)	SMAD2	100.3	108.2	113.7	1.1	1.1
NM_005902	SMAD, mothers against DPP homolog 3 (*Drosophila*)	SMAD3	110.2	106.5	127.7	1.0	1.2
BF526175	SMAD, mothers against DPP homolog 5 (*Drosophila*)	**SMAD5**	361.0	488.3	514.2	1.4	1.4
AI478523	SMAD, mothers against DPP homolog 5 (*Drosophila*)	SMAD5	300.7	384.9	346.9	1.3	1.2
AF010601	SMAD, mothers against DPP homolog 5 (*Drosophila*)	SMAD5	79.2	99.7	87.6	1.3	1.1
AY014180	SMAD-specific E3 ubiquitin protein ligase 2	SMURF2	804.2	844.7	851.8	1.1	1.1
AU157259	SMAD-specific E3 ubiquitin protein ligase 2	SMURF2	77.1	81.5	86.3	1.1	1.1
AL575922	Secreted protein, acidic, cysteine-rich (osteonectin)	**SPARC**	1702.1	1935.5	1925.8	1.1	1.1
BF508662	Sprouty homolog 1, antagonist of FGF signaling (*Drosophila*)	SPRY1	31.9	46.3	45.4	1.5	1.4
NM_014886	TGF beta-inducible nuclear protein 1	TINP1	1185.7	1259.5	1241.1	1.1	1.0

C, vehicle control; D, 5α-dihydrotestosterone; Ex, exemestane. Genes that performed quantitative RT-PCR were described in bold style.

steroidal aromatase inhibitor, has been therefore attributed to its actions through AR in osteoblasts. Systemic androgenic effects such as hypertricosis, hair loss, hoarseness, and acne have been reported only in 4% [6] of the patients treated with EXE (25 mg/day) and the frequency of these effects increases to approximately 10% in those treated with higher dose 200 mg/day of EXE [6]. This finding suggests that the patients treated with EXE are under relatively weak systemic androgenic effects. Androgen sensitivity has been well-known to be subject to great individual variation caused by AR gene CAG polymorphism in women as well as men [29,30]. Therefore, this 5 to 10% of the patients who manifested clinical androgenic effects by EXE treatment may be individuals associated with relatively enhanced androgenic sensitivity. Replacement therapy with TST is generally effective at restoring bone in hypogonadal men [31]. In female-to-male, genetic female transsexual subjects, high-dose TST therapy generally increased BMD at the femoral neck, despite decrement of E2 to postmenopausal levels [32,33]. Therefore, androgens may play an important role in bone protection in women as well as men.

The results of cell proliferation assay demonstrated that the cell number of MG-63 was increased by both E2 and DHT treatments, but the dose of DHT was relatively higher than that in two other cells. MG-63 expressed higher levels of ERα/β mRNA, but the level of AR mRNA was lower than that in both Saos-2 and hFOB. Both cell proliferation and ALP activity of MG-63 could not be stimulated by EXE treatment. Molecular mechanisms of androgen actions on osteoblasts have remained largely unknown. Androgen is well-known to stimulate osteoblast proliferation [34] and differentiation [35]. For instance, osteoprotegerin mRNA was increased by TST as well as DHT treatments in mouse 3T3-E1 cells [36].

AR and ERβ but not ERα are predominantly detected in osteoblasts located on human cancellous bone using immunohistochemical analysis [37]. Therefore, hFOB examined in this study is considered to maintain relatively native status of sex steroids pathways in human osteoblasts. Therefore, we employed hFOB for further examination of EXE effects on osteoblast gene expression pattern using microarray analysis. In this study, we demonstrated that the genes MYBL2 [38], OSTM1 [39], HOXD11 [40], ADCYAP1R1 [41], and GPC2 [42] were target genes of EXE alone or both EXE and DHT in hFOB using microarray/PCR analysis. These genes were demonstrated to be involved in regulation of cell cycle, differentiation, and transcription. In EXE or DHT treatment in hFOB and Saos-2, in which cells proliferations were stimulated, an increased expression of HOXD11 gene was detected. The product of the mouse Hoxd11 gene was reported to play a role in forelimb morphogenesis [40,43]. Therefore, these finding suggest that osteoblast cell proliferation stimulated by EXE treatment may depend on HOXD11 gene expression through AR. In this study, the cell proliferation of MG-63, which expressed relatively low level of AR, was not stimulated by EXE. In addition, HOXD11 gene expression was not up-regulated by EXE treatment in MG-63 cells. These results were also consist with the protective effects of EXE through potential androgen-HOXD11 pathway in osteoblast cells. In this study, we also examined the effects of EXE and DHT on osteoblast growth-related genes using micro-

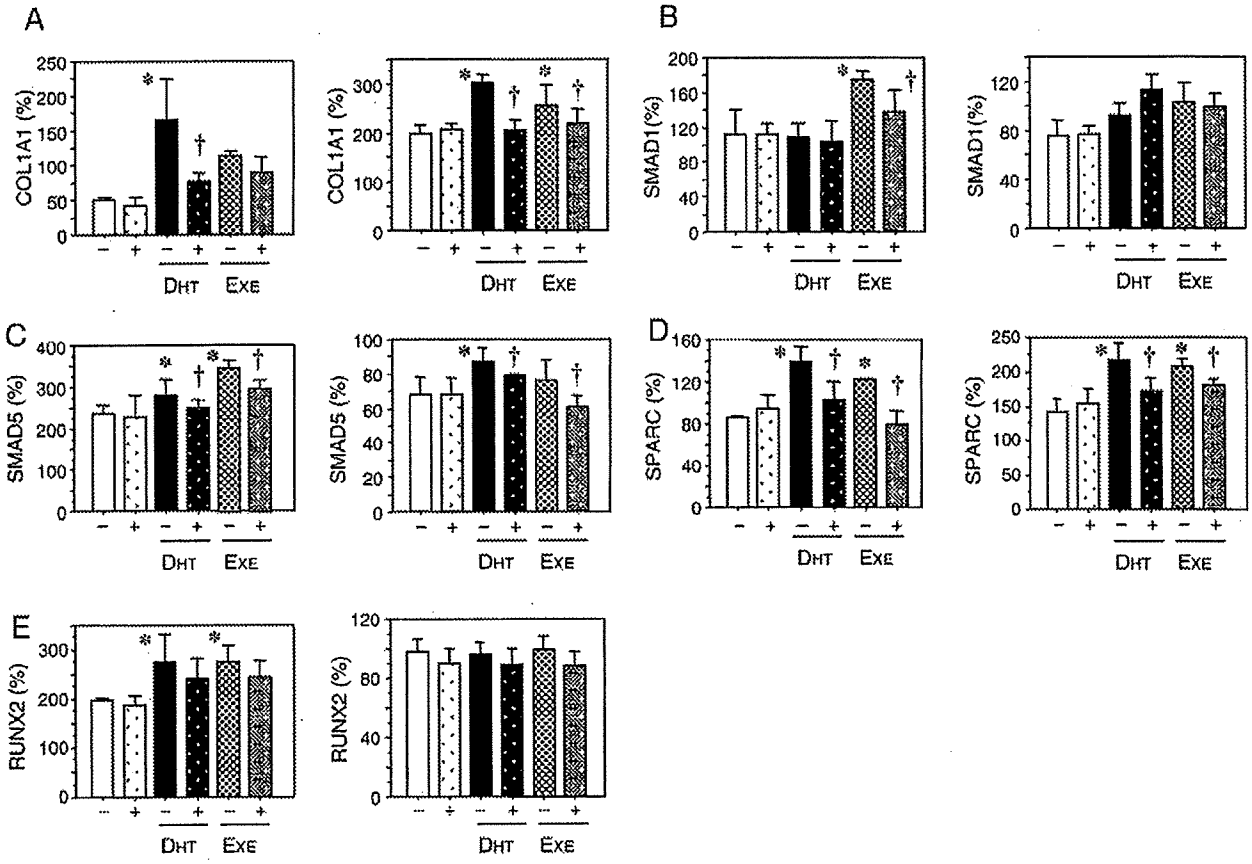

Fig. 7. Expression levels of osteoblast growth-related genes in hFOB (left) and Saos-2 (right). DHT: 10^{-8} M 5α-dihydrotestosterone, EXE: 10^{-7} M Exemestane, with (+) or without (−) hydroxyflutamide, $p<0.05$ vs. control (*) or without hydroxyflutamide (†).

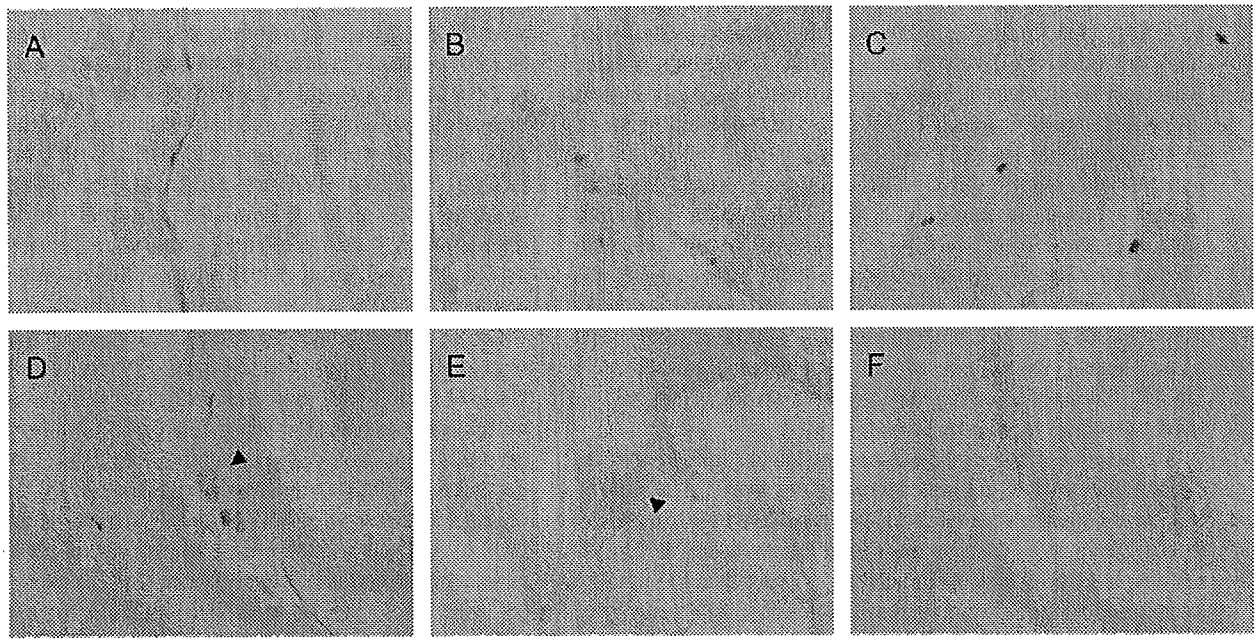

Fig. 8. Immunohistochemistry of androgen receptor in human bone tissues. Immunoreactivity of androgen receptor was detected in nuclei of osteoblasts/liner cells (A, B) but not in osteoclasts (D, E; arrowheads). Immunoreactivity of androgen receptor was also detected in nuclei of osteocytes (C) and condrocytes (F).

array analysis and following quantitative RT-PCR. COL1A1, SMAD5, and SPARC (osteonectine) were up-regulated by EXE and/or DHT treatments in both hFOB and Saos-2 cells. EXE or DHT treatments in both hFOB and Saos-2 also resulted in increased ALP activity. There have been, however, no studies reported on whether these genes are primary or secondary androgen responsive genes in osteoblasts. The AR-specific antagonist, OHF demonstrated no inhibitory effects on RUNX2 expression increased by EXE or DHT treatment in hFOB cells. In addition, hFOB cell growth induced by high dose of EXE treatment was not completely inhibited by OHF treatment. These results all suggest that EXE also may stimulate hFOB cell proliferation through both AR dependent and independent pathways. From our data of steroid production in hFOB, EXE may have an additional androgenic effect through increased TST levels in conjunction with inhibition of aromatization in hFOB cells. However, it awaits further investigations for clarification.

In normal bone remodeling, bone formation by osteoblasts follows bone resorption by osteoclasts and occurs in a precise and quantitative manner (coupling). In this coupling between bone formation and resorption, a coupling factor that induces bone formation is considered to be released during osteoclastic bone resorption [44]. This study has focused on the specific effects on osteoblast cells. However, it is true that there were significant increases in both serum bone formation and resorption markers in postmenopausal women administered with EXE for 2 years [26]. Osteoclasts, which are responsible for bone resorption, are target cells for many anti-osteoporosis therapeutic agents such as bisphosphonate of postmenopausal women [45]. However, it is unclear whether EXE acts on osteoclast directly. Chen et al. [46] reported that testosterone inhibited osteoclast formation stimulated by parathyroid hormone through the AR but not through the production of intrinsic estrogen using primary mouse osteoclast cells. In both human and rodent bone tissues, AR is expressed in both osteoblasts and osteocytes [47,48]. However, AR is detected in osteoclasts of rodent but not in human cells [31,47,48]. Therefore, in humans, androgens are considered to exert their effects on bone through osteoblasts. EXE may therefore exert its possible androgenic effects on human bone through osteoblasts but not osteoclasts. Results of our present study also suggest the possible roles of EXE on osteoblast cells through AR independent manner. Results of clinical studies suggest that the combination therapy of AI and COX-2 inhibitors could provide more effective aromatase inhibition than single therapy in hormone-sensitive postmenopausal breast cancer [49]. Bone resorption induced by IL-1 and IL-6 was also reported to occur via stimulation of COX-2 dependent PGE_2 production in osteoblasts *in vitro* [50]. Therefore, further investigations are required to clarify the effects of AI including EXE on human bone tissues.

In summary, this study using osteoblast and osteoblast-like cell lines suggested the potential protective effect of steroidal AI, EXE on osteoblasts occurred through both AR dependent and independent pathways. HOXD11 gene known as bone morphogenesis factor and osteoblast growth-related genes were induced by EXE treatment as well as DHT treatment in both hFOB and Saos-2. Damages of bone tissues by estrogen depletion caused by AI administration are considered unavoidable but the selection of potential hormone therapies which could minimize the damages or injuries of bone tissues is considered important.

Acknowledgments

We appreciate Dr. Shin-ichi Hayashi (Divisions of Molecular Medical Technology, Tohoku University School of Medicine) for critical comments. We also appreciate Ms. Chika Tazawa, Ms. Toshie Suzuki, Ms. Miki Mori and Mr. Katsuhiko Ono (Department of Pathology, Tohoku University School of Medicine) for skillful technical assistances. This research was supported by Grant-in-aid for Health and Labor Sciences Research Grant on Risk of Chemical Substances (H16-Kagaku-002) from Ministry of Health, Labor, and Welfare, Japan and Kanzawa Medical Research Foundation, Nagano, Japan.

References

[1] Rogers J. Estrogens in the menopause and postmenopause. N Engl J Med 1969;280:364–7.
[2] Wingate L. The epidemiology of osteoporosis. J Med 1984;15:245–66.
[3] Felson DT, Zhang Y, Hannan MT, Kiel DP, Wilson PW, Anderson JJ. The effect of postmenopausal estrogen therapy on bone density in elderly women. N Engl J Med 1993;329:1141–6.
[4] Lester L, Coleman R. Bone loss and the aromatase inhibitors. Br J Cancer 2005;93:S16–22.
[5] Miller WR, Dixon JM. Antiaromatase agents: preclinical data and neoadjuvant therapy. Clin Breast Cancer 2000;1:S9–S14.
[6] Lønning PE, Paridaens R, Thurlimann B, Piscitelli G, di Salle E. Exemestane experience in breast cancer treatment. J Steroid Biochem Mol Biol 1997;61:151–5.
[7] Center for Drug Evaluation and Research Application Number NDA 20753 (Exemestane) Medical Review. Food and Drug Administration, 1999.
[8] Goss PE, Qi S, Josse RG, Pritzker KPH, Mendes M, Hu H, et al. The steroidal Aromatase inhibitor exemestane prevent bone loss in ovariectomized rats. Bone 2004;34:384–92.
[9] Goss PE, Qi S, Cheung AM, Hu H, Mendes M, Pritzker KPH. Effects of steroidal aromatase inhibitor exemestane and the nonsteroidal aromatase inhibitor letrozole on bone and lipid metabolism in the ovariectomized rats. Clin Cancer Res 2004;10:5717–23.
[10] Sasano H, Uzuki M, Sawai T, Nagura H, Matsunaga G, Kashimoto O, et al. Aromatase in human bone tissue. J Bone Miner Res 1997;12:1416–23.
[11] Schweikert HU, Wolf L, Romalo G. Oestrogen formation from Androstendione in human bone. Clin Endocrinol 1995;43:37–42.
[12] Purohit A, Flanagan AM, Reed MJ. Estrogen synthesis by osteoblast cell lines. Endocrinology 1992;131:2027–9.
[13] Tanaka S, Haji M, Nishi Y, Yanase T, Takayanagi R, Nawata H. Aromatase activity in human osteoblast-like osteosarcoma cell. Calcif Tissue Int 1993;52:107–9.
[14] Recanatini M, Bisi A, Cavalli A, Belluti F, Gobbi S, Rampa A, et al. A new class of nonsteroidal aromatase inhibitors: design and synthesis of chromone and xanthone derivatives and inhibition of the P450 enzymes aromatase and 17 alpha-hydroxylase/C17,20-lyase. J Med Chem 2001;44:672–80.
[15] Linkhart TA, Mohan S, Baylink DJ. Growth factors for bone growth and repair: IGF, TGF beta and BMP. Bone 1996;19:1S–12S.
[16] Harris SA, Enger RJ, Riggs BL, Spelsberg TC. Development and characterization of a conditionally immortalized human fetal osteoblastic cell line. J Bone Miner Res 1995;10:178–86.
[17] Suzuki T, Darnel AD, Akahira JI, Ariga N, Ogawa S, Kaneko C, et al. 5alpha-reductases in human breast carcinoma: possible modulator of in situ androgenic actions. J Clin Endocrinol Metab 2001;86:2250–7.

[18] Miki Y, Suzuki T, Tazawa C, Ishizuka M, Semba S, Gorai I, et al. Analysis of gene expression induced by diethylstilbestrol (DES) in human primitive Müllerian duct cells using microarray. Cancer Lett 2005;220:197–210.
[19] Yamamoto M, Takahashi Y, Tabata Y. Controlled release by biodegradable hydrogels enhances the ectopic bone formation of bone morphogenetic protein. Biomaterials 2003;24:4375–83.
[20] Kanno J, Aisaki K, Igarashi K, Nakatsu N, Ono A, Kodama Y, et al. "Per cell" normalization method for mRNA measurement by quantitative PCR and microarrays. BMC Genomics 2006;29:64.
[21] Eisen MB, Spellman PT, Brown PO, Bostein D. Cluster analysis and display of genome-wide expression patterns. Proc Natl Acad Sci U S A 1998;95:14863–8.
[22] Miki Y, Nakata T, Suzuki T, Darnel AD, Moriya T, Kaneko C, et al. Systemic distribution of steroid sulfatase and estrogen sulfotransferase in human adult and fetal tissues. J Clin Endcrinol Metab 2002;87:5760–8.
[23] Ishizuka M, Hatori M, Suzuki T, Miki Y, Darnel AD, Tazawa C, et al. Sex steroid receptors in rheumatoid arthritis. Clin Sci (Lond) 2004;106: 293–300.
[24] Rodan GA, Noda M. Gene expression in osteoblastic cells. Crit Rev Eukaryot Gene Expr 1991;1:85–98.
[25] Ito Y, Miyazono K. RUNX transcription factors as key role of TGF-β superfamily signaling. Curr Opin Genet Dev 2003;13:43–7.
[26] Lønning PE, Geisler J, Krag LE, Erikstein B, Bremnes Y, Hagen AI, et al. Effects of exemestane administered for 2 years versus placebo on bone mineral density, bone biomarkers, and plasma lipids in patients with surgically respected early breast cancer. J Clin Oncol 2005;23:4847–9.
[27] Coombes RC, Hall E, Gibson LJ, Paridaens R, Jassem J, Delozier T, et al. Intergroup Exemestane Study. A randomized trial of exemestane after two to three years of tamoxifen therapy in postmenopausal women with primary breast cancer. N Engl J Med 2004;350:1081–92.
[28] Coleman RE, Banks LM, Girgis SI, Vrdoljak E, Fox J, Porter LS, et al. Skeletal effect of exemestane in the Intergroup Exemestane Study (IES)—2 years bone mineral density (BMD) and bone biomarker data. Breast Cancer Res Treat 2005;94:S233.
[29] Vottero A, Stratalis CA, Ghizzoni L, Longui CA, Karl M, Chrousos GP. Androgen receptor-mediated hypersensitivity to androgen in women with nonhyperandrogenic hirsutism: skewing of X-chromosome inactivation. J Clin Endocrinol Metab 1999;84:1091–5.
[30] Brum IS, Spritzer PM, Paris F, Maturana MA, Audran F, Sultan C. Association between androgen receptor gene CAG repeat polymorphism and plasma testosterone levels in postmenopausal women. J Soc Gynecol Investig 2005;12:135–41.
[31] Vanderschueren D, Vandenput L, Boonen S, Lindberg MK, Bouillon R, Ohlsson C. Androgens and bone. Endocr Rev 2004;25:389–425.
[32] Turner A, Chen T, Barber T, Malabanan A, Holick M, Tangpricha V. Testosterone increases bone mineral density in female-to-male transsexuals: a case series of 15 subjects. Clin Endocrinol (Oxf) 2004;61:560–6.
[33] Ruetsche AG, Kneubuehl R, Birkhaeuser MH, Lippuner K. Cortical and trabecular bone mineral density in transsexuals after long-term cross-sex hormonal treatment: a cross-sectional study. Osteoporos Int 2005;16: 791–98.
[34] Kasperk CH, Wergedal JE, Farley JR, Linkhart TA, Turner RT, Baylink DJ. Androgens directly stimulate proliferation of bone cells in vitro. Endocrinology 1989;124:1576–8.
[35] Kasperk C, Fitzsimmons R, Strong D, Mohan S, Jennings J, Wergedal J, et al. Studies of the mechanism by which androgens enhance mitogenesis and differentiation in bone cells. J Clin Endocrinol Metab 1990;71:1322–9.
[36] Chen Q, Kaji H, Kanatani M, Sugimoto T, Chihara K. Testosterone increases osteoprotegerin mRNA expression in mouse osteoblast cells. Horm Metab Res 2004;36:674–8.
[37] Bord S, Horner A, Beavan S, Compston J. Estrogen receptors alpha and beta are differentially expressed in developing human bone. J Clin Endocrinol Metab 2001;86:2309–14.
[38] Sala A, Watson R. B-Myb protein in cellular proliferation, transcription control, and cancer: latest developments. J Cell Physiol 1999;179:245–50.
[39] Chalhoub N, Benachenhou N, Rajapurohitam V, Pata M, Ferron M, Frattini A, et al. Grey-lethal mutation induces severe malignant autosomal recessive osteopetrosis in mouse and human. Nat Med 2003;9:399–406.
[40] Boulet AM, Capecchi MR. Multiple roles of Hoxa11 and Hoxd11 in the formation of the mammalian forelimb zeugopod. Development 2004; 131:299–309.
[41] Lundberg P, Lundgren I, Mukohyama H, Lehenkari PP, Horton MA, Lerner UH. Vasoactive intestinal peptide (VIP)/pituitary adenylate cyclase-activating peptide receptor subtypes in mouse calvarial osteoblasts: presence of VIP-2 receptors and differentiation-induced expression of VIP-1 receptors. Endocrinology 2001;142:339–47.
[42] Gutierrez J, Osses N, Brandan E. Changes in secreted and cell associated proteoglycan synthesis during conversion of myoblasts to osteoblasts in response to bone morphogenetic protein-2: role of decorin in cell response to BMP-2. J Cell Physiol 2006;206:58–67.
[43] Omi M, Fisher M, Maihle NJ, Dealy CN. Studies on epidermal growth factor receptor signaling in vertebrate limb patterning. Dev Dyn 2005;233:288–300.
[44] Rodan GA, Raisz LG, Bilezikian JP. Pathophysiology of osteoporosis. . (chapter 73)In: Bilezikian JP, Raisz LG, Rodan GA, editors. Principles of bone biology, 2nd ed., vol. 1. NY, USA: Academic Press, A division of Harcourt, Inc.; 2002. p. 1275–90.
[45] Kellinsalmi M, Monkkonen H, Monkkonen J, Leskela HV, Parikka V, Hamalainen M, et al. In vitro comparison of clodronate, pamidronate and zoledronic acid effects on rat osteoclasts and human stem cell-derived osteoblasts. Basic Clin Pharmacol Toxicol 2005;97:382–91.
[46] Chen Q, Kaji H, Sugimoto T, Chihara K. Testosterone inhibits osteoclast formation stimulated by parathyroid hormone through androgen receptor. FEBS Lett 2001;491:91–3.
[47] Abu EO, Horner A, Kusec V, Triffitt JT, Compston JE. The localization of androgen receptors in human bone. J Clin Endocrinol Metab 1997; 82:3493–7.
[48] Wiren KM, Orwoll ES. Androgens: receptor expression and steroid action in bone. . (chapter 43)In: Bilezikian JP, Raisz LG, Rodan GA, editors. Principles of bone biology, 2nd ed., vol. 1. NY, USA: Academic Press, A division of Harcourt, Inc.; 2002. p. 757–72.
[49] Chow LW, Wong JL, Toi M. Celecoxib anti-aromatase neoadjuvant (CAAN) trial for locally advanced breast cancer: preliminary report. J Steroid Biochem Mol Biol 2003;86:443–7.
[50] Sato T, Morita I, Sakaguchi K, Nakahama KI, Smith WL, Dewitt DL, et al. Involvement of prostaglandin endoperoxide H synthase-2 in osteoclast-like cell formation induced by interleukin-1 beta. J Bone Miner Res 1996;11:392–400.

0888-8809/06/$15.00/0
Printed in U.S.A.

Molecular Endocrinology 20(9):2141–2155

doi: 10.1210/me.2005-0367

Endocrine-Disrupting Organotin Compounds Are Potent Inducers of Adipogenesis in Vertebrates

Felix Grün, Hajime Watanabe, Zamaneh Zamanian, Lauren Maeda, Kayo Arima, Ryan Cubacha, David M. Gardiner, Jun Kanno, Taisen Iguchi, and Bruce Blumberg

Department of Developmental and Cell Biology (F.G., Z.Z., L.M., K.A., R.C., D.M.G., B.B.), University of California Irvine, Irvine California 92697-2300; National Institutes of Natural Sciences (H.W., T.I.), National Institute for Basic Biology, Okazaki Institute for Integrative Bioscience, Okazaki 444-8787, Japan; and Division of Cellular & Molecular Toxicology (J.K.), Biological Safety Research Center, National Institute of Health Sciences, Setagaya-ku, Tokyo 158-8501, Japan

Dietary and xenobiotic compounds can disrupt endocrine signaling, particularly of steroid receptors and sexual differentiation. Evidence is also mounting that implicates environmental agents in the growing epidemic of obesity. Despite a long-standing interest in such compounds, their identity has remained elusive. Here we show that the persistent and ubiquitous environmental contaminant, tributyltin chloride (TBT), induces the differentiation of adipocytes *in vitro* and increases adipose mass *in vivo*. TBT is a dual, nanomolar affinity ligand for both the retinoid X receptor (RXR) and the peroxisome proliferator-activated receptor γ (PPARγ). TBT promotes adipogenesis in the murine 3T3-L1 cell model and perturbs key regulators of adipogenesis and lipogenic pathways *in vivo*. Moreover, *in utero* exposure to TBT leads to strikingly elevated lipid accumulation in adipose depots, liver, and testis of neonate mice and results in increased epididymal adipose mass in adults. In the amphibian *Xenopus laevis*, ectopic adipocytes form in and around gonadal tissues after organotin, RXR, or PPARγ ligand exposure. TBT represents, to our knowledge, the first example of an environmental endocrine disrupter that promotes adipogenesis through RXR and PPARγ activation. Developmental or chronic lifetime exposure to organotins may therefore act as a chemical stressor for obesity and related disorders. (*Molecular Endocrinology* 20: 2141–2155, 2006)

ORGANOTINS ARE A diverse group of widely distributed environmental pollutants. Tributyltin chloride (TBT) and bis(triphenyltin) oxide (TPTO), have pleiotropic adverse effects on both invertebrate and vertebrate endocrine systems. Organotins were first used in the 1960s as antifouling agents in marine shipping paints, although such use has been restricted in recent years. Organotins persist as prevalent contaminants in dietary sources, such as fish and shellfish, and through pesticide use on high-value food crops (1, 2). Additional human exposure to organotins may occur through their use as antifungal agents in wood treatments, industrial water systems, and textiles. Mono- and diorganotins are prevalently used as stabilizers in the manufacture of polyolefin plastics (polyvinyl chloride), which introduces the potential for transfer by contact with drinking water and foods.

Exposure to organotins such as TBT and TPTO results in imposex, the abnormal induction of male sex characteristics in female gastropod mollusks (3, 4). Bioaccumulation of organotins decreases aromatase activity leading to a rise in testosterone levels that promotes development of male characteristics (5). Imposex results in impaired reproductive fitness or sterility in the affected animals and is one of the clearest examples of environmental endocrine disruption. TBT exposure also leads to masculinization of at least two fish species (6, 7), but TBT is only reported to have modest adverse effects on mammalian male and female reproductive tracts and does not alter sex ratios (8, 9). Instead, hepatic-, neuro-, and immunotoxicity appear to be the predominant effects of organotin exposure (10). Hence, the current mechanistic understanding of the endocrine-disrupting potential of organotins is based on their direct actions on the levels or activity of key steroid-regulatory enzymes such as aromatase and more general toxicity mediated via damage to mitochondrial functions and subsequent cellular stress responses (11–15).

However, it remains an open question whether *in vivo* organotins act primarily as protein and enzyme

First Published Online April 13, 2006

Abbreviations: Acac, Acetyl-coenzyme A carboxylase; b.w., body weight; C/EBP, CCAAT/enhancer binding protein; 9-*cis* RA, 9-cis retinoic acid; DMSO, dimethylsulfoxide; F, forward; Fatp, fatty acid transport protein; LBD, ligand-binding domain; LXR, liver X receptor; MDIT, 3-isobutyl-1-methylxanthine, dexamethasone, insulin and T_3 adipocyte differentiation mix; PPAR, peroxisome proliferator-activated receptor; R, reverse; RAR, retinoic acid receptor; RXR, retinoid X receptor; Srebf1, sterol-regulatory element binding factor 1; TBT, tributyltin chloride; TPTO, triphenyltin oxide; TTNPB, (E)-4-[2-(5,6,7,8-tetrahydro-5,5,8,8-tetramethyl-2-naphthylenyl)-1-propenyl] benzoic acid; VDR, vitamin D receptor.

***Molecular Endocrinology* is published monthly by The Endocrine Society (http://www.endo-society.org), the foremost professional society serving the endocrine community.**

inhibitors, or rather mediate their endocrine-disrupting effects at the transcriptional level. Recent work has shown that aromatase mRNA levels can be down-regulated in human ovarian granulosa cells by treatment with organotins or ligands for the nuclear hormone receptors, retinoid X receptor (RXRs) or peroxisome proliferator-activated receptor γ (PPARγ) (16–18). Furthermore, Nishikawa *et al.* (19) have demonstrated that the gastropod *Thais clavigara* RXR homolog is responsive to 9-cis-retinoic acid (9-*cis*-RA) and TBT, and 9-*cis* RA can also induce imposex, suggesting a conserved transcriptional mechanism for TBT action across phyla. These ligand-dependent transcription factors belong to the nuclear hormone receptor superfamily—a group of approximately 150 members (48 human genes) that includes the estrogen receptor, androgen receptor, glucocorticoid receptor, thyroid hormone receptor, vitamin D receptor (VDR), retinoic acid receptors (RARs and RXRs), PPARs, and numerous orphan receptors. We were therefore intrigued by the similar effects of TBT and RXR/PPARγ ligands on mammalian aromatase mRNA expression and hypothesized that TBT might be exerting some of its biological effects via transcriptional regulation of gene expression through activation of one or more nuclear hormone receptors.

Our results show that organotins such as TBT are indeed potent and efficacious agonistic ligands of the vertebrate nuclear receptors, retinoid X receptors (RXRs) and PPARγ. The physiological consequences of receptor activation predict that permissive RXR heterodimer target genes and downstream signaling cascades are sensitive to organotin misregulation. Consistent with this prediction we observe that organotins phenocopy the effects of RXR and PPARγ ligands using *in vitro* and *in vivo* models of adipogenesis. Therefore, TBT and related organotin compounds are the first of a potentially new class of environmental endocrine disrupters that targets adipogenesis by modulating the activity of key regulatory transcription factors in the adipogenic pathway, RXRα and PPARγ. The existence of such xenobiotic compounds was previously hypothesized (20, 21). Our results suggest that developmental exposure to TBT and its congeners that activate RXR/PPARγ might be expected to increase the incidence of obesity in exposed individuals and that chronic lifetime exposure could act as a potential chemical stressor for obesity and obesity-related disorders.

RESULTS

Organotins Are Agonists of Vertebrate RXR and RXR-Permissive Heterodimers

Many known or suspected environmental endocrine-disrupting chemicals mimic natural lipophilic hormones that act through members of the superfamily of nuclear receptor transcription factors (22, 23). In a screen of high-priority endocrine-disrupting chemicals against a bank of vertebrate nuclear receptor ligand-binding domains (LBDs), we observed that organotins, specifically tributyltin chloride (TBT) and bis(triphenyltin) oxide (TPTO), could fully activate an RXRα LBD construct (GAL4-RXRα) in transient transfection assays. Both TBT and TPTO were as potent (EC_{50} ~3–10 nM) as 9-*cis* retinoic acid, an endogenous RXR ligand and approximately 2- to 5-fold less potent than the synthetic RXR-specific ligands LG100268 (EC_{50} ~ 2 nM) or AGN195203 (EC_{50} ~ 0.5 nM) (Fig. 1A and see Table 2). Maximal activation for TBT reached the same levels as LG100268 or AGN195203.

We next tested whether activation by TBT was unique to RXRα only, restricted to RXR heterodimer complexes, or a general nuclear receptor transcriptional response (Fig. 1, B–D, and Table 1). TBT activated RXRα and RXRγ from the amphibian *Xenopus laevis* in addition to human RXRs (Table 1). Our results are consistent with recent findings by Nishikawa *et al.* (19, 24) that organotins promote activation of all three human RXR subtypes in a yeast two-hybrid screen. We also observed significant activation of receptors typically considered to be permissive heterodimeric partners of RXR including human PPARγ (Fig. 1B, ~30% maximal activation of 10 μM troglitazone, but note that activation is compromised by cellular toxicity above 100 nM), PPARδ, liver X receptor (LXR), and the orphan receptor NURR1. In contrast, typical nonpermissive partners such as RARs, thyroid hormone receptor, and VDR failed to show activation by organotins (Fig. 1C and Table 1). Murine PPARα was also not activated by TBT although it was fully activated by its specific synthetic agonist WY-14643 (Fig. 1D). The steroid and xenobiotic receptor was likewise unresponsive. The orphan receptor NURR1, which has no discernable ligand pocket and is believed to be ligand independent (25), was nevertheless activated 7- to 10-fold at 100 nM TBT. Similarly, other RXR-specific ligands, *e.g.* LG100268, activated NURR1 to the same degree, suggesting that this response occurred through NURR1's heterodimeric partner RXR as has been previously described (25, 26). Like other RXR-specific ligands, tributyltin was also able to promote the ligand-dependent recruitment of nuclear receptor cofactors such as receptor-associated coactivator 3 (ACTR), steroid receptor coactivator-1, and PPAR-binding protein in mammalian two-hybrid interaction assays (data not shown). We infer from these results that nuclear receptor activation by TBT activation is specific to a small subset of receptors and not a consequence of a general effect on the cellular transcriptional machinery.

We next investigated the relationship between the structure of the tin compounds and RXR activation by testing the response of GAL4-RXRα to mono-, di-, tri-, and tetra-substituted butyltin, branched side chains, variations in the alkyl chain length, and changes in the halide component (Fig. 1A and Table 2). Overall, trialkyltin compounds were the most effective with nano-

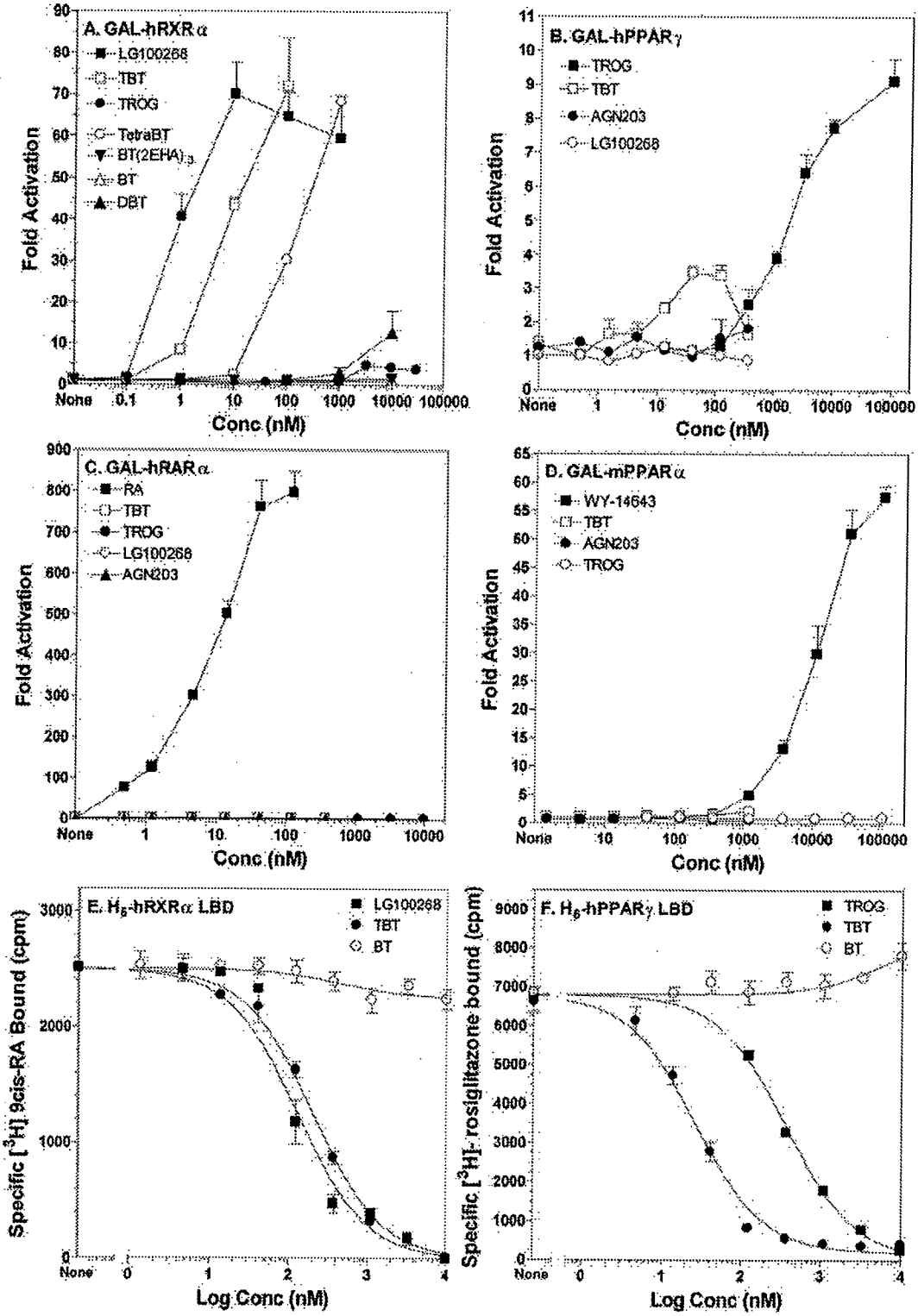

Fig. 1. Organotins Are Agonist Ligands of RXRα and PPARγ

Organotins are high-affinity ligand agonists of RXRα and PPARγ. A–D, Activation of GAL4-hRXRα, -hPPARγ, -hRARα, or -hPPARα in transiently transfected Cos7 cells by organotins and receptor-specific ligands. Data represent reporter luciferase activity normalized to β-galactosidase and plotted as the average fold activation ± SEM (n = 3) relative to solvent-only controls from representative experiments. E and F, Competition binding curves of histidine-tagged RXRα or PPARγ LBDs with TBT. Data shown are from a representative experiment analyzed in GraphPad Prism 4.0 and K_i values deduced (Table 3). Conc, Concentration; DBT, dibutyltin chloride; TROG, troglitazone.

Table 1. TBT Activates RXRs and RXR-Permissive Heterodimers

GAL4-NR LBD	Fold Activation at 60 nM TBT	Permissive RXR Heterodimer
RXRα (*Homo sapiens*)	60	Yes
RXRα (*X. laevis*)	25	Yes
RXRγ (*X. laevis*)	7.0	Yes
NURR1 (*H. sapiens*)	7.0	Yes
LXR (*H. sapiens*)	2.1	Yes
PPARα (*Mus musculus*)	0.7	Yes
PPARγ (*H. sapiens*)	5.3	Yes
PPARδ (*H. sapiens*)	1.7	Yes
RARα (*H. sapiens*)	0.7	No
TR&β (*H. sapiens*)	0.4	No
VDR (*H. sapiens*)	0.5	No
SXR (*H. sapiens*)	1.0	No

Data are fold activation at 60 nM TBT relative to solvent-only controls of transiently transfected Cos7 cells after 24 h ligand treatment. SXR, Steroid and xenobiotic receptor; TR, thyroid hormone receptor.

molar EC_{50} values. Monobutyltin gave no significant activation whereas dibutyltin was moderately active in the micromolar range (Fig. 1A and Table 2). Tetrabutyltin was 20-fold less potent than TBT, whereas the branched side-chain butyltin tris(2-ethylhexanoate) [BT(2-EHA)$_3$] was inactive (Table 2). Although activation by dialkyltins is weaker than that of TBT, it is potentially significant due to their widespread use in the manufacture of polyvinyl chloride plastics and greater solubility than TBT.

The effect of the hydrocarbon chain length was very pronounced, suggesting an important structure-activity relationship. A reduction in hydrophobicity from butyl to ethyl side chains raised the EC_{50} value by almost 1000-fold into the micromolar range. Trimethyltin was weakly active only above 100 μM (Table 2). Substitution of the halide component had no significant effect on the EC_{50} values for TBT, probably due to the lability of the halide atom through exchange in aqueous tissue culture media where chloride ions are prevalent.

Table 2. Organotin EC_{50} Values for Nuclear Receptor LBDs

Ligand	GAL4-NR LBD Transactivation (EC_{50} Values, nM)		
	hRXRα	hRARα	hPPARγ
LGD268	2–5	na	na
AGN195203	0.5–2	na	na
9-*cis* RA	15	na	na
all-*trans* RA	na	8	na
Butyltin chloride	na	na	na
Dibutyltin chloride	3000	na	na
TBT	3–8	na	20
Tetrabutyltin	150	ND	ND
Di(triphenyltin)oxide	2–10	na	20
Butyltin tris(2-ethylhexanoate)	na	ND	ND
Troglitazone	na	na	1000
Tributyltin fluoride	3	ND	ND
Tributyltin bromide	4	ND	ND
Tributyltin iodide	4	ND	ND
Triethyltin bromide	2800	ND	ND
Trimethyltin chloride	>10000	ND	ND

na, Not active; ND, not determined. EC_{50} values were determined from dose-response curves of GAL4-NR LBD construct activation in transiently transfected Cos7 cells after 24-h ligand exposure.

TBT Is a Potent Ligand of Both RXRα and PPARγ

Many, if not most, natural and synthetic nuclear receptor agonists act as ligands that specifically interact with their cognate receptor LBDs. We therefore performed equilibrium competition binding experiments with purified histidine-tagged human RXRα (H_6-RXRα) and PPARγ (H_6-PPARγ) LBDs to determine whether the potent and specific activation of these receptors by TBT was due to direct ligand-receptor interaction (Fig. 1, E and F).

The equilibrium binding curves indicate that TBT is a high-affinity, competitive ligand for 9-*cis* RA-bound RXRα. The inhibition equilibrium dissociation constant was calculated by the Chang-Prusoff method [inhibition constant (K_i) = dissociation constant (K_d)] as 12.5 nM (10–15 nM; 95% confidence interval) (Table 3). By comparison, the value obtained for the synthetic RXR agonist LG100268 was 7.5 nM, which compared favorably with its published value of approximately 3 ± 1 nM (27). Therefore, the identification of TBT as an RXR ligand expands the molecular definition of known rexinoids (agonists able to activate RXR) to include this structurally unique class of organotin compounds.

Somewhat surprisingly, we also observed potent specific competitive binding by TBT for rosiglitazone bound to human PPARγ LBD (Fig. 2B). The deduced K_i of 20 nM (17–40 nM; 95% confidence interval) was slightly higher than for RXRα but significantly better than the K_i for the PPARγ agonist troglitazone, which

Table 3. TBT Binding Constants (K_d) for hRXRα and hPPARγ LBDs

Ligand	Receptor Competitive Inhibition Binding Constants K_i (nM ± 95% CI)		
	H_6-RXRα	H_6-PPARγ	Published
TBT	12.5 (10–15)	20 (17–40)	
LG100268	7.5 (6–10)	ND	3 ± 1[a]
Troglitazone	ND	300 (270–335)	300 ± 30[b]

Competition binding curves were determined at constant ^{3}H-specific ligand concentrations [20 nM 9-*cis*-RA, K_d = 1.4 nM (87) or rosiglitazone, K_d = 41 nM (88)] with increasing cold competitor ligands over the range indicated in Fig. 1, E and F. Data were analyzed in GraphPad Prism by nonlinear regression of a competitive one-site binding equation (Chang-Prusoff method) to determine K_i values ± 95% confidence intervals (n = 3). CI, Confidence interval; ND, not determined.
[a] RXRα:LG100268 K_d = 3 ± 1 nM (27).
[b] PPARγ:troglitazone K_d = 300 ± 30 nM (28).

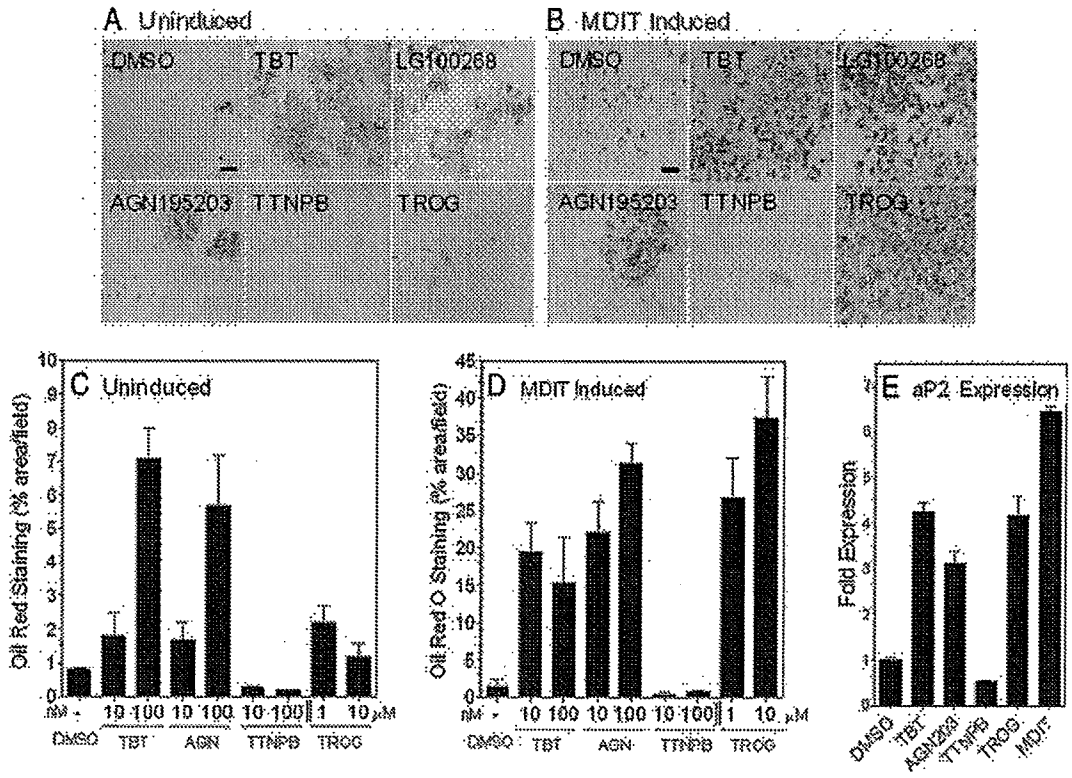

Fig. 2. Tributyltin Induces Adipogenesis in 3T3-L1 Cells

Uninduced (A) and MDIT-induced (B) 3T3-L1 cultures grown for 1 wk in the presence of vehicle (DMSO), or ligands were analyzed for mature adipocyte differentiation by Oil Red O staining. *Scale bar* represents 100 μm. C and D, The percentage area stained was determined by automated analysis of random fields (n = 9) from high-contrast dissecting scope photographs of monolayers analyzed in ImageJ; 1–100 nM of TBT, AGN195203, and TTNPB or 1–10 μM troglitazone. E, Quantitative real-time PCR (QRT-PCR) of adipocyte-specific fatty acid binding protein aP2 (aP2/Fabp4) expression levels in postconfluent 3T3-L1 cells treated with the indicated ligands for 24 h. Data were normalized to glyceraldehyde-3-phosphate dehydrogenase controls and plotted as average fold induction ± SEM (n = 3).TROG, Troglitazone.

yielded a K_i of 300 nM, consistent with its published K_d (28). The K_d values for TBT binding to RXRα (12.5 nM) and PPARγ (20 nM) are also in close agreement with EC_{50} values obtained from transient transfection assays using GAL4-RXRα and GAL4-PPARγ constructs (Table 2).

Taken together, these data show that organotins such as TBT, although structurally distinct from previously described natural or synthetic ligands, can interact with RXRα and PPARγ, via direct ligand binding to induce productive receptor-coactivator interactions and promote transcription in a concentration-dependent manner. Organotins are therefore potent nanomolar receptor activators on par with synthetic RXR and PPARγ ligands such as LG100268, AGN195203, and thiazolidinediones.

TBT Promotes Adipogenesis in the Murine 3T3-L1 Cell (Embryonic Murine Preadipocyte Fibroblast Cell Line) Model

Numerous studies have demonstrated the critical role played by RXRα:PPARγ signaling in regulation of mammalian adipogenesis (29–31). In the murine 3T3-L1 preadipocyte cell model, adipogenic signals induce early key transcriptional regulators such as CCAAT/enhancer binding proteins (C/EBPs) β and δ that lead to mitotic clonal expansion of growth-arrested preadipocytes and induction of the late differentiation factors C/EBPα and PPARγ (32–34). The combination of C/EBPα expression together with PPARγ signaling efficiently drives terminal adipocyte differentiation and lipid accumulation. We therefore tested whether TBT signaling through RXR:PPARγ could promote adipogenesis in the murine 3T3-L1 differentiation assay and compared its effect to other RXR-specific or PPARγ ligands (Fig. 2). Undifferentiated 3T3-L1 cells were cultured for 1 wk in the presence of ligands either with or without a prior 2-d treatment with MDIT (an adipogenic-sensitizing cocktail of 3-isobutyl-1-methylxanthine, dexamethasone, insulin, and T_3) (35). Cells were then scored for lipid accumulation using Oil Red O staining to determine the degree of terminal adipocyte differentiation. TBT was as effective as LG100268 or AGN195203 in promoting dif-

ferentiation in the absence of MDIT treatment, increasing the number of differentiated adipocytes about 7-fold over solvent-only controls (Fig. 2, A and C). The PPARγ agonist troglitazone was a weak inducer in the absence of MDIT. Prior treatment with MDIT increased the response to TBT, LG100268, and AGN195203 a further 3- to 5-fold (Fig. 2, B and D). MDIT treatment also boosted the response to troglitazone to equivalent levels as expected from published studies showing that combination treatment with PPARγ ligands promotes efficient adipocyte differentiation (36–38). In contrast, the RAR agonist TTNPB inhibited the differentiation of 3T3-L1 cells, consistent with previously published data that showed RAR signaling blocks adipogenesis during the early stages of differentiation *in vitro* and can modulate adiposity and whole body weight *in vivo* (39–41). The differential response of 3T3-L1 cells to receptor-selective retinoids indicates that TBT favors RXR homodimer or permissive RXR-heterodimer rather than RXR:RAR signaling in this cell model.

Adipocyte differentiation by TBT was accompanied by direct transcriptional effects on RXR:PPARγ targets such as adipocyte-specific fatty acid-binding protein (aP2) mRNA. The aP2 promoter contains response elements sensitive to C/EBP factors and RXRα:PPARγ signaling (42). Quantitative real-time PCR analysis showed aP2 levels were elevated by TBT treatment approximately 5-fold at 24 h (Fig. 2E) and 45-fold at 72 h (data not shown). LG100268, troglitazone, and MDIT treatment also increased aP2 expression at these time points whereas the RAR agonist TTNPB was inhibitory, consistent with the observed cellular responses.

TBT Induces Adipogenic Regulators and Markers of RXRα:PPARγ Signaling *in Vivo*

The ability of organotins to regulate RXRα:PPARγ target genes and key modulators of adipogenesis and lipid homeostasis *in vivo* has not been previously examined. Therefore, we next asked whether TBT could perturb expression of critical transcriptional mediators of adipogenesis such as RXRα, PPARγ, C/EBPα/β/δ, and sterol regulatory element binding factor 1 (Srebf1) as well as known target genes of RXRα:PPARγ signaling from liver, epididymal adipose tissue, and testis of 6-wk-old male mice dosed for 24 h with TBT [0.3 mg/kg body weight (b.w.)], AGN195203 (0.3 mg/kg b.w.), troglitazone (3 mg/kg b.w), or vehicle (corn oil) administered by ip injection. TBT either had no effect or weakly repressed RXRα and PPARγ transcription in liver (Fig. 3, A and B). A more pronounced decrease was observed for RXRα, PPARγ, C/EBPα, and C/EBPδ in adipose tissue and testis (Fig. 3, B and C). In contrast, TBT, AGN195203, and troglitazone significantly induced expression of the early adipogenic transcription factor C/EBPβ in liver and testis, whereas it was more weakly induced in adipose tissue. Induction was strongest in testis where TBT and troglitazone increased expression greater than 10-fold and AGN195203 increased expression 60-fold compared with vehicle controls (Fig. 3C). In addition to C/EBPβ, the proadipogenic transcription factor Srebf1 was also significantly increased in adipose tissue by all three receptor ligands and weakly induced in liver.

We also observed coordinate changes in several well-characterized direct target genes of RXR:PPARγ signaling. Fatty acid transport protein (Fatp) acts as a key control point for regulation of cellular fatty acid content. The Fatp promoter contains a functional PPAR response element shown to be sensitive to RXR:PPARγ signaling in 3T3-L1 adipocytes and white fat (43–46). Fatp mRNA levels were up regulated 2- to 3-fold in liver and epididymal adipose tissue but not testis by TBT, AGN195203, and troglitazone (see Fig. 5, A and B). Similarly, the PPARγ target phosphoenolpyruvate carboxykinase 1 (PEPCK/Pck1) (47), the rate-limiting step in hepatic gluconeogenesis and adipose glyceroneogenesis, was up-regulated in liver and adipose tissues by TBT or troglitazone treatment.

Signaling through RXR:PPARγ, RXR:LXR, and ADD1/Srebf1 in hepatocytes has been shown to modulate fatty acid synthesis through transcriptional control of acetyl-coenzyme A carboxylase (Acac), the rate-limiting step in long-chain fatty acid synthesis (48, 49), as well as fatty acid synthase (Fasn) (50–53). Hepatic expression of both Acac and Fasn was unregulated between 1.5–2.5-fold by TBT, AGN195203, and troglitazone. Therefore, the coordinate increased expression of Fatp, Pck1, Acac, and Fasn in liver suggests that TBT stimulates fatty acid uptake and triglyceride synthesis. Similar changes have been reported in the induction of hepatic steatosis by overactive PPARγ signaling (49, 54).

Taken together, these data show that TBT exposure induces lipogenic RXR:PPARγ target gene expression, in adipose tissue and liver, and modulates associated early adipocyte differentiation factors such as C/EBPβ and Srebf1. We inferred from these data that organotins are potential adipogenic agents *in vivo*.

Developmental Exposure to TBT Disrupts Lipid Homeostasis and Adipogenesis in Vertebrates

Based on its molecular pharmacology, ability to induce 3T3-L1 adipocyte differentiation, and *in vivo* transcriptional responses, we reasoned that TBT would disrupt normal endocrine control over lipid homeostasis and impact adipogenesis, particularly when exposure occurred during sensitive periods of development. We therefore tested this hypothesis in two vertebrate model systems, mouse and *X. laevis*, during embryogenesis.

Pregnant C57BL/6 mice were injected daily from gestational d 12–18 with TBT (0.05 or 0.5 mg/kg body weight ip) dissolved in sesame oil or vehicle alone. Pups were then killed at birth, and histological sections were prepared from liver, testis, mammary gland, and inguinal adipose tissue. Sections were stained